Evaluation of the 24th Street Bridge

BRIDGE ENGINEERING CENTER

Final Report
November 2010

IOWA STATE UNIVERSITY
Institute for Transportation

Sponsored by
Federal Highway Administration
Iowa Department of Transportation

About the BEC

The mission of the Bridge Engineering Center is to conduct research on bridge technologies to help bridge designers/owners design, build, and maintain long-lasting bridges.

Disclaimer Notice

The contents of this report reflect the views of the authors, who are responsible for the facts and the accuracy of the information presented herein. The opinions, findings and conclusions expressed in this publication are those of the authors and not necessarily those of the sponsors.

The sponsors assume no liability for the contents or use of the information contained in this document. This report does not constitute a standard, specification, or regulation.

The sponsors do not endorse products or manufacturers. Trademarks or manufacturers' names appear in this report only because they are considered essential to the objective of the document.

Non-discrimination Statement

Iowa State University does not discriminate on the basis of race, color, age, religion, national origin, sexual orientation, gender identity, sex, marital status, disability, or status as a U.S. veteran. Inquiries can be directed to the Director of Equal Opportunity and Diversity, (515) 294-7612.

Iowa Department of Transportation Statements

Federal and state laws prohibit employment and/or public accommodation discrimination on the basis of age, color, creed, disability, gender identity, national origin, pregnancy, race, religion, sex, sexual orientation or veteran's status. If you believe you have been discriminated against, please contact the Iowa Civil Rights Commission at 800-457-4416 or Iowa Department of Transportation's affirmative action officer. If you need accommodations because of a disability to access the Iowa Department of Transportation's services, contact the agency's affirmative action officer at 800-262-0003.

The preparation of this (report, document, etc.) was financed in part through funds provided by the Iowa Department of Transportation through its "Agreement for the Management of Research Conducted by Iowa State University for the Iowa Department of Transportation," and its amendments.

The opinions, findings, and conclusions expressed in this publication are those of the authors and not necessarily those of the Iowa Department of Transportation.

Technical Report Documentation Page

1. Report No.	2. Government Accession No.	3. Recipient's Catalog No.

4. Title and Subtitle	5. Report Date
Evaluation of the 24th Street Bridge	November 2010
	6. Performing Organization Code

7. Author(s)	8. Performing Organization Report No.
Terry Wipf, Brent Phares, Jake Bigelow, Travis Hosteng, and Anna Nadermann	

9. Performing Organization Name and Address	10. Work Unit No. (TRAIS)
Institute for Transportation Iowa State University 2711 South Loop Drive, Suite 4700 Ames, IA 50010-8664	11. Contract or Grant No.

12. Sponsoring Organization Name and Address	13. Type of Report and Period Covered
Federal Highway Administration 1200 New Jersey Avenue SE Washington, DC 20590 Iowa Department of Transportation 800 Lincoln Way Ames, IA 50010	14. Sponsoring Agency Code

15. Supplementary Notes

Funding provided though the Federal Highway Administration (FHWA) Innovative Bridge Research and Construction (IBRC) and Highways for LIFE (HfL). The Iowa Department of Transportation (DOT) received the FHWA funds directly and contracted with Iowa State University.

16. Abstract

Using accelerated construction methods, a prestressed, precast bridge, was constructed the by Iowa DOT. The design concept involved the use of precast deck components that were grouted compositely with the steel girders. The successful implementation of this approach has far reaching implications in Iowa as well as nationwide, as there are many instances where proven rapid construction techniques could result in significant reductions in costs.

The overall objective of this project was to assess bridge components and evaluate the overall performance of the 24th Street bridge. In order to complete the objective the project included laboratory test and field testing. The laboratory test included evaluating the shear stud pockets, (including the stud bend test and grout flowability), evaluation of duct splicing performance, and the influence of surface treatment on transverse joint shear transfer. The field test included monitoring strand corrosion, deck panel behavior during placement, post-tensioning strand behavior, and a diagnostic live load test.

17. Key Words	18. Distribution Statement
accelerated bridge construction evaluation—bridge construction lab and field testing—cost-effective precast bridge construction—precast bridge deck panels	No restrictions.

19. Security Classification (of this report)	20. Security Classification (of this page)	21. No. of Pages	22. Price
Unclassified.	Unclassified.	54	NA

Form DOT F 1700.7 (8-72) **Reproduction of completed page authorized**

EVALUATION OF THE 24TH STREET BRIDGE

Final Report
November 2010

Co-Principal Investigator
Terry J. Wipf
Director, Bridge Engineering Center
Institute for Transportation, Iowa State University

Co-Principal Investigator
Brent M. Phares
Associate Director, Bridge Engineering Center
Institute for Transportation, Iowa State University

Authors
Terry Wipf, Brent Phares, Jake Bigelow, Travis Hosteng, and Anna Nadermann

Sponsored by
The Iowa Department of Transportation
Office of Bridges and Structures

Preparation of this report was financed in part
through funds provided by the Iowa Department of Transportation.

A report from
Institute for Transportation
Iowa State University
2711 South Loop Drive, Suite 4700
Ames, IA 50010-8664
Phone: 515-294-8103
Fax: 515-294-0467
www.intrans.iastate.edu

TABLE OF CONTENTS

ACKNOWLEDGMENTS IX

EXECUTIVE SUMMARY XI

1. GENERAL INFORMATION 1

1.1. Introduction 1
1.2. Background 1
1.3. Objectives & Scope 2

2. BRIDGE DESCRIPTION 3

3. LABORATORY TESTING 9

3.1. Shear Stud: Shear Stud Pocket Investigation 9
3.2. Evaluation of Duct Splicing Performance 10
3.3. Evaluation of the Influence of Surface Treatment on Transverse Joint 11
3.4. Lab Testing Key Findings 13

4. FIELD TESTING 13

4.1. Strand Corrosion Monitoring 13
4.2. Deck Panel Behavior during Handling 15
4.3. Post-tensioning Strand Behavior during Stressing 26
4.4. Diagnostic Live Load Testing 28
4.5. Field Testing Key Findings 39

5. SUMMARY AND CONCLUSIONS 40

REFERENCES 42

LIST OF FIGURES

Figure 1.1. Boone County precast concrete deck panel (Wipf, et al. 2009) 2
Figure 2.1. Construction of south abutment and terrace walls 3
Figure 2.2. Girders on west center pier during Phase I construction 4
Figure 2.3. Girder ends at field splice location 4
Figure 2.4. Girder layout and elevation 5
Figure 2.5. Placing precast deck panel on girders 5
Figure 2.6. Precast panel layout 6
Figure 2.7. Precast deck panel configuration 7
Figure 2.8. Shear stud pocket and studs 8
Figure 3.1. Stud pocket and haunch mockup after form removal 9
Figure 3.2. Mockup splice connections for 1 in. x 3 in. P-T duct 10
Figure 3.3. Push-out tests for transverse joint surface treatment 11
Figure 3.4. Deflection vs. Load plot for sandblasted specimen #3 11
Figure 4.1. Corrosion electrode tied to strand 13
Figure 4.2. Location of strands monitored for corrosion at north abutment 14
Figure 4.3. Strain gauge layout on precast deck panels 16
Figure 4.4. Precast deck panel in construction staging yard ready for placement 17
Figure 4.5. Deck panel being lifted into place 17
Figure 4.6. Final maneuvering of precast deck panel placement 18
Figure 4.7. Strain gauge orientation for each gauge line 19
Figure 4.8. Panel No. 1 strain readings during panel placement 21
Figure 4.9. Strain profile along gridlines A, B, and C, Panel No. 1 22
Figure 4.10. Panel No. 2 strain readings during placement 24
Figure 4.11. Strain profile along gridlines D, E, and F, Panel No. 2 25
Figure 4.12. Location of load cells in precast deck panels 26
Figure 4.13. Final installation of load cell in deck joint (top view) 26
Figure 4.14. Deck panel load during strand stressing 27
Figure 4.15. Gauge location on bridge 28
Figure 4.16. Cross-sectional strain gauge configurations 29
Figure 4.17. Truck load paths (truck traveled north into the page) 29
Figure 4.18. 2008 truck axle loads 30
Figure 4.19. Representative time history deflections for Load Case 2 30
Figure 4.20. Representative time history strain at pier bottom flange load location, Load Case 2 31
Figure 4.21. Representative time history strain at mid-span bottom flange load location, Load Case 2 32
Figure 4.22. Representative time history strain at abutment bottom flange load location, Load Case 2 32
Figure 4.23. Girder J cross-section strain, Load Case 2 33
Figure 4.24. Load Case 5 girder deflection and differential movement at closure pour 34
Figure 4.25. Load Case 6 girder deflection and differential movement at closure pour 34
Figure 4.26. Experimentally-obtained load fraction for six load cases 35
Figure 4.27. Load fractions combined to form load distribution 36
Figure 4.28. Experimental and codified load distributions 36

Figure 4.29. Strain depth profile for girders G through J, Load Case 2 37
Figure 4.30. Strain depth profile for girders G through J, Load Case 3 38

LIST OF TABLES

Table 4.1. Vetek V2000 electrode readings.....14
Table 4.2. V2000 millivolt electrode readings.....15
Table 4.3. Range of strain at various locations.....33

ACKNOWLEDGMENTS

This research was sponsored by the Federal Highway Administration (FHWA) Innovative Bridge Research and Construction (IBRC) and Highways for LIFE (HfL). The authors would like to thank Doug Wood for his help in installing monitoring equipment and conducting the testing. The authors would like to thank Coreslab Structures, Cramer and Associates, and VSL for their insight and cooperation during testing. The authors would also like to thank the Iowa Department of Transportation (DOT) workers that helped with the load test of the bridge.

EXECUTIVE SUMMARY

Using accelerated construction methods, a prestressed, precast bridge, was constructed the by Iowa Department of Transportation (DOT). The design concept involved the use of precast deck components that were grouted compositely with the steel girders. The successful implementation of this approach has far reaching implications in Iowa as well as nationwide, as there are many instances where proven rapid construction techniques could result in significant reductions in costs.

The overall objective of this project was to assess bridge components and evaluate the overall performance of the 24th Street Bridge. In order to complete the objective, the project included laboratory test and field testing. The laboratory test included evaluating the shear stud pockets, (including the stud bend test and grout flowability), evaluation of duct splicing performance, and the influence of surface treatment on transverse joint shear transfer. The field test included monitoring strand corrosion, deck panel behavior during placement, post-tensioning strand behavior, and a diagnostic live load test.

The following conclusions were obtained during the testing:

1. No difficulty in installing the shear studs in the precast panel pockets were foreseen by the contractor or encountered by the research team.
2. Conducting the bend test on the studs in the precast panel pockets was feasible for all six studs.
3. Grout with the proposed slump can sufficiently flow through the stud pockets into the haunch areas.
4. The waterproof duct tape and butyl rubber methods of grout proofing the duct splices were both acceptable.
5. Sandblasting the surface of the concrete/grout joint was the most effective surface treatment for resistance to shear.
6. All corrosion electrodes indicate that no corrosion is taking place in the strands.
7. During deck panel placement the peak strain in the panel was 230 με located at F2, which was near a pick point location.
8. The maximum north span deflection was observed to be -0.41 in., which corresponds to a span to deflection ration of L/5120.
9. The maximum strain of +66 με occurred at the midspan of girder L during LC1. The maximum strain range of 88 με occurred at the same location and load case.
10. The largest load distribution factor was found at girder H with a value of 0.63. The lowest load distribution factor of 0.30 occurred at girder A.
11. The load distribution factors obtained from field testing were within the American Association of State Highway and Transportation Officials (AASHTO) Load and Resistance Factor Design (LRFD) load distribution requirements.
12. The neutral axis location obtained from field test was located between 58 in. and 61 in. form the bottom of the flange. The girder depth is 61 in.; therefore the neutral axis lies near the top of the steel girder but not in the haunch or deck slab.

1. GENERAL INFORMATION

1.1. Introduction

Recently, there has been increased interest in constructing bridges that last longer, are less expensive, and take less time to construct. The idea is to generally increase the cost-effectiveness of bridges by increasing their durability (i.e., useful life) and minimizing disruptions to the traveling public. Clearly there is much to learn about how to best accomplish this nationally important goal. Although there may be many ways to achieve it, currently, one of the most commonly discussed ideas include using some form of precast, segmental construction. This type of construction has the advantage that the individual components are manufactured off-site where increased quality is usually achieved. Further, because much of the work is completed away from the bridge site, it is anticipated that user disruptions would be minimized since the amount of labor intensive on-site work would be reduced which leads to reduced on-site construction time.

Using accelerated construction methods, a prestressed, precast bridge, was constructed by the Iowa Department of Transportation (DOT). The design concept involved the use of precast deck components that were grouted compositely with the steel girders. The successful implementation of this approach has far reaching implications in Iowa as well as nationwide, as there are many instances where proven rapid construction techniques could result in significant reductions in costs. The application of precast deck panels represents a step forward from previous systems in Iowa and strives to further improve the design concept. This report documents the 24th Street Bridge including laboratory testing and field testing of the bridge.

1.2. Background

In 2006 (Wipf, et al. 2009) the Iowa DOT and Iowa Highway Research Board (IHRB) constructed one of the first accelerated precast deck bridges in the state in Boone County, Iowa. The precast deck for the bridge was 16 ft-1 in. transversely and 8 ft- 1 in. longitudinally. The deck has eight transverse prestressing strands and transverse #7 bars located at the opening were the deck is grouted to the girders. The grout openings run the full longitudinal length of the deck. Figure 1.1 shows the Boone County deck panel. The development of the 24th street bridge deck panels evolved from the knowledge learned during the design, fabrication, and construction of the Boone County Bridge.

Figure 1.1. Boone County precast concrete deck panel (Wipf, et al. 2009)

The successful implementation of the 24th Street Bridge project has far reaching implications in the State of Iowa as it will allow for continuation of developmental work initiated through previous Innovative Bridge Research and Construction (IBRC) program projects. This project directly addresses the Highway for Life (HfL) initiative and the Innovative Bridge Research and Deployment (IBRD) (AbuHawash et al. 2007) program goals of demonstrating (and documenting) the effectiveness of innovative construction techniques for the construction of new bridge structures.

1.3. Objectives & Scope

The overall objective of this project was to perform laboratory and field tests to evaluate the 24th Street Bridge components and assess the bridges overall performance.

To satisfy the objectives, the project scope included the following tasks:

- Investigate the installation and testing of the shear studs
- Evaluation of material consolidation in shear stud pocket
- Evaluation of the influence of surface treatment on transverse joint shear transfer
- Evaluation of duct splicing performance
- Monitoring for corrosion of prestress and post-tensioning strands
- Deck panel behavior during handling
- Post-tensioning strand behavior during stressing
- Diagnostic live load testing

2. BRIDGE DESCRIPTION

The 24th Street Bridge was constructed in two phases at an existing bridge site. The west lanes were constructed during Phase I of the project and the east lanes were constructed during Phase II. The new bridge carries six lanes of 24th street traffic (four through lanes and 2 turning lanes) over Interstate 80 in Council Bluffs, IA. The bridge is two spans with a total length of 353 ft-6 in. from center-line of abutment bearings. The south and north spans are 178 ft-6 in. and 175 ft-0 in. respectively. The girders are continuous over the center support and simply supported at the abutments. The abutments consist of one row of vertical piling and one row of battered piling with a concrete cap and backwall. The spill through slope is terraced down to the road level as shown in Figure 2.1. The center pier has two rows of vertical piling support with a continuous concrete pier cap shown in Figure 2.2.

The superstructure of the 24th Street Bridge is comprised of prestressed precast deck panels supported and composite with steel plate girders. The completed bridge has 12 lines of girders spaced at 9 ft-0 in. on center. The girders have a depth of approximately 60 in. The flange thickness varies from 1 in. near the abutments to 2 in. at the pier. Each girder has two bolted field splices with a maximum girder length between splices of 121.75 ft. Figure 2.3 shows the girder ends at the field splice location. Figure 2.4 shows the structural steel layout of the superstructure and a girder elevation view (the label system of the girder layout is used throughout the document).

Figure 2.1. Construction of south abutment and terrace walls

Figure 2.2. Girders on west center pier during Phase I construction

Figure 2.3. Girder ends at field splice location

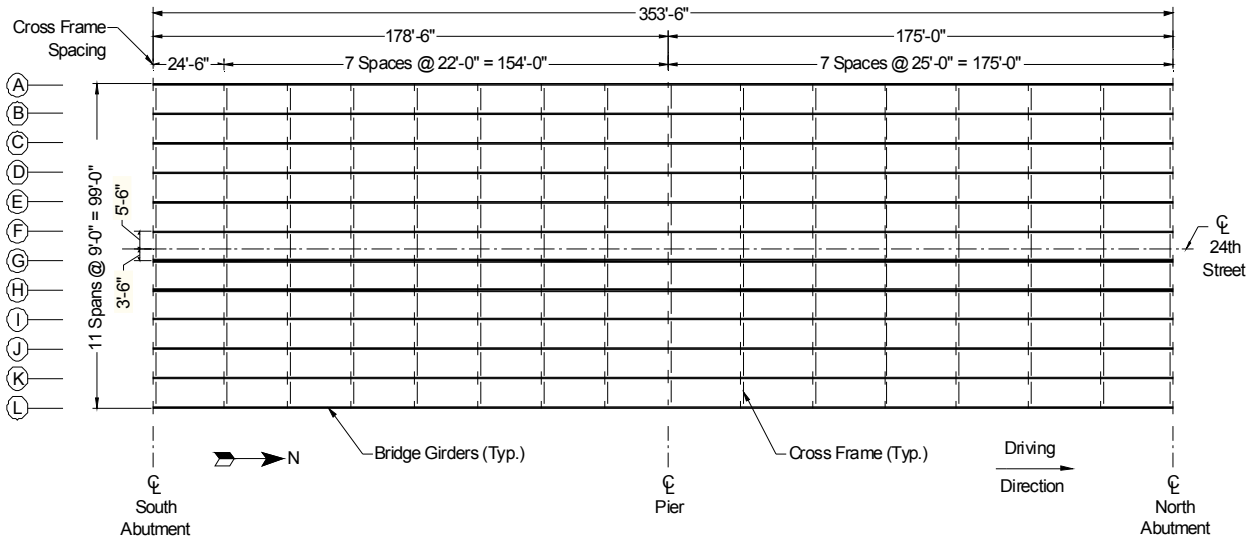

Figure 2.4. Girder layout and elevation

The precast deck panels, being placed in Figure 2.5, were designed to act compositely with the girders, requiring the deck be connected to the girders through the use of shear connectors. The deck panels are 10 ft long x 52 ft-4 in. wide x 8 in. thick. The deck panel layout is shown in Figure 2.6. Each panel has 28 1 in. by 3 in. embedded ducts to house four longitudinal post-tensioning strands which run the full length of the bridge. Each panel is transversely prestressed with 10 1/2 in. dia. strands. Figure 2.7 shows the schematic of the typical precast deck panel. The deck to girder composite action was obtained with the use of 1 ft 4 in. by 11 in. shear stud pockets in the precast panels as shown in Figure 2.8. Shear studs were welded on the girder within the "pockets" of the panels; the "pockets" were then filled with grout.

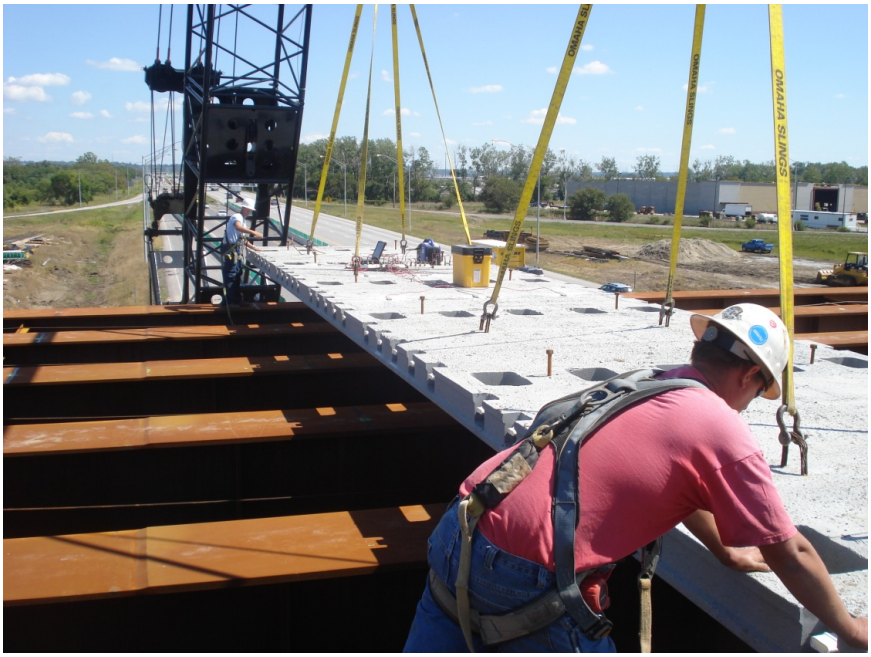

Figure 2.5. Placing precast deck panel on girders

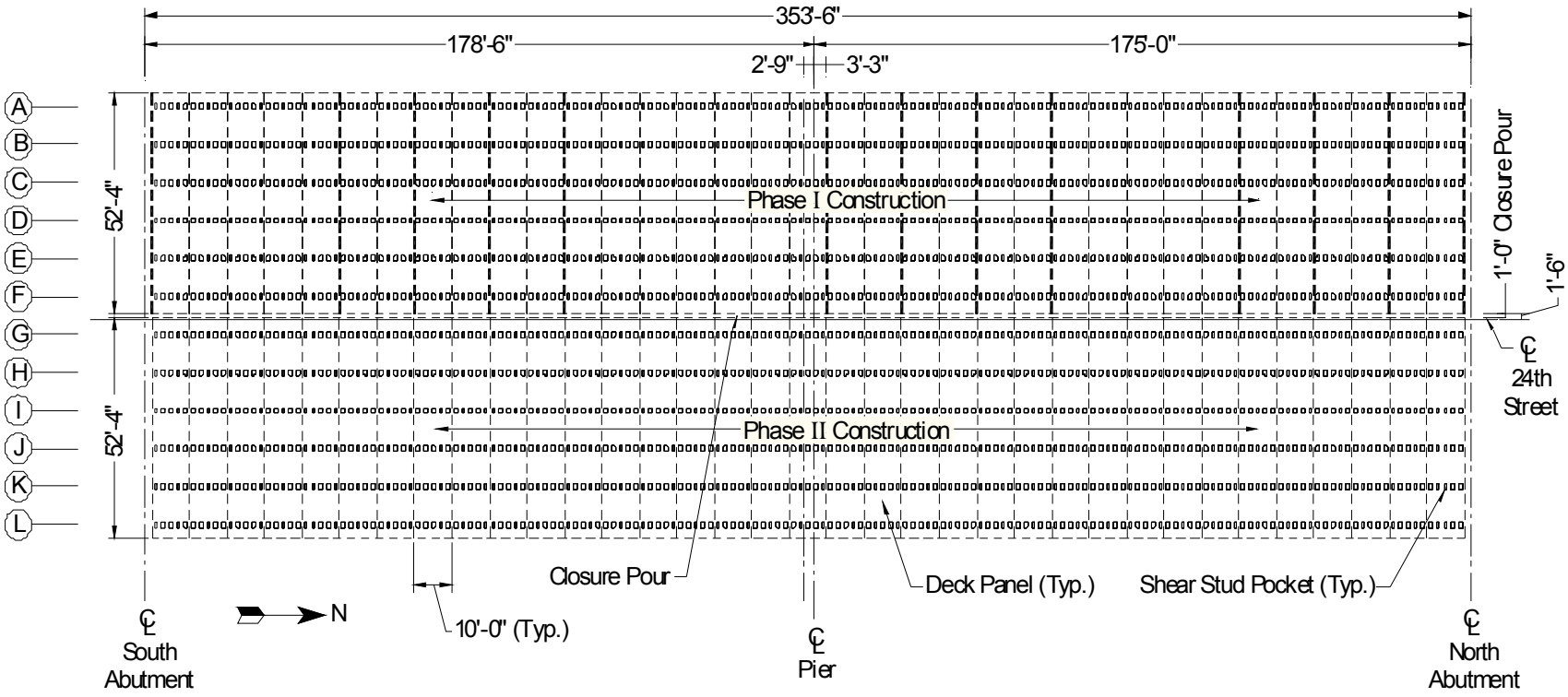

Figure 2.6. Precast panel layout

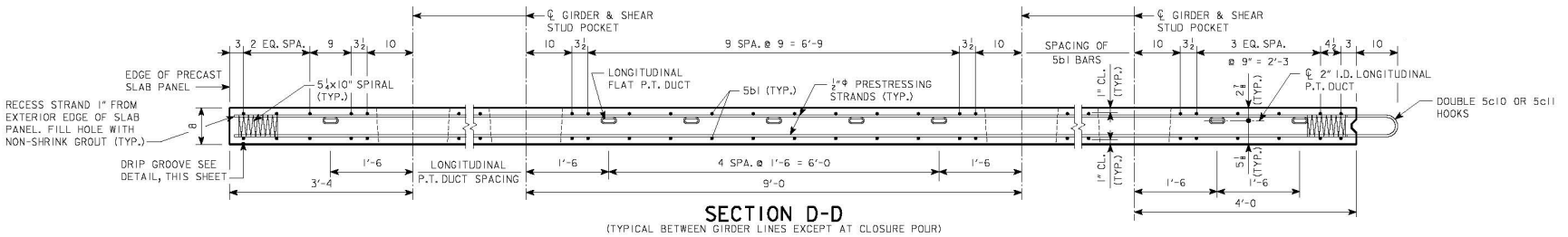

a. Precast slab transverse section

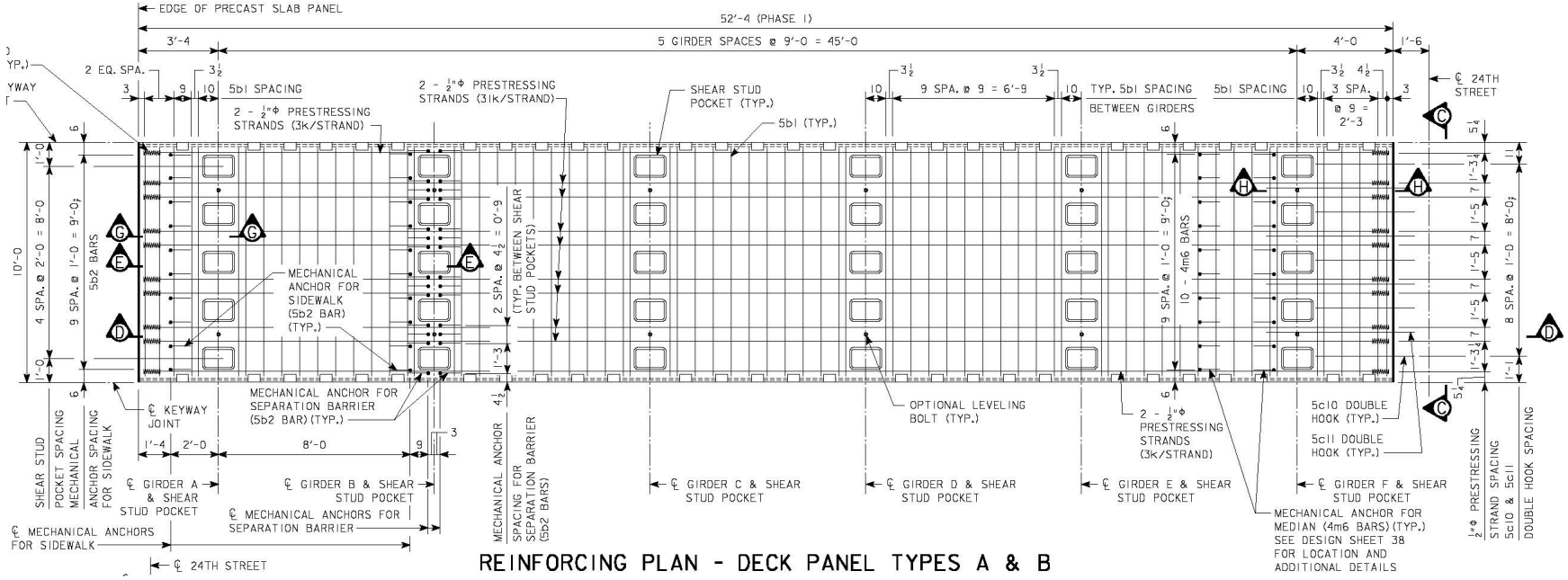

b. Precast slab plan

Figure 2.7. Precast deck panel configuration

Figure 2.8. Shear stud pocket and studs

3. LABORATORY TESTING

Three laboratory tests were conducted prior to the fabrication and construction of the bridge. The test involved a shear stud pocket investigation, duct splice performance, and transverse joint treatment. The results of the three test were used to recommend fabrication and construction techniques for the bridge.

3.1. Shear Stud: Shear Stud Pocket Investigation

The bridge design called for shear studs to be welded to the top flange of the superstructure girders, within the preformed deck panel pockets. Installing the shear studs and performing bend test within the pocket was a constructability concern, therefore a mockup of two successive stud pockets was created out of plywood with a piece of plate steel simulating the beam top flange. In addition, the mockup was used to investigate the grouts ability to flow into the haunch between the precast panels and the steel girder top flanges. The haunch was taken as the minimum haunch, which was approximately 2 in.

No difficulty was found in bending the four studs in the corners of the stud pocket. Bending of the center two studs was more arduous but still possible. The grout was then placed into the two stud pockets in the mockup and agitated with an electric vibrator. Figure 3.1 shows the mockup after removal of the forms, clearly indicating that grout can sufficiently flow through the stud pockets and into the haunch area in the specified dimensions. The grout, however, did have small air pockets/voids that formed on the surface as seen in Figure 3.1b. It is uncertain how the air pocket would affect the long term performance of the haunch grout.

During construction of the panels the precaster had difficulty finding an economical blockout form during casting of the panel. The tapered edges of the pocket as seen in Figure 3.1 were eliminated and the sides of the blockout were redesigned to be vertical in order to provide cost savings to the project.

a. Grout filled pockets and haunch **b. Close up of grout at haunch**

Figure 3.1. Stud pocket and haunch mockup after form removal

3.2. Evaluation of Duct Splicing Performance

In order to longitudinally post-tension the deck panels, ducts are installed in the deck panels which must then be connected in the field prior to stringing the post-tensioning strands. The design requires the ducts in adjacent precast panels be joined by a duct coupler and be sealed with a waterproof covering in order to protect the ducts from infiltration of grout when the transverse joints are cast. To test the integrity of this coupler and waterproof covering, a mockup of the system was made and the performance verified.

The 1in. x 3in. duct splice connection detail was evaluated to determine if grout or moisture would seep into the duct at the connection. Two mockup duct splices were constructed and placed in grout. One duct splice was constructed of Polyken waterproof duct tape, as shown in Figure 3.2a. The second splice mockup was constructed with butyl rubber strips wrapped around the joint interfaces of the duct and coupler, the longitudinal joint of the coupler was sealed with a strip of Polyken duct tape, as shown in Figure 3.2b. Both methods of grout proofing the splices were found acceptable.

a. Waterproof duct tape

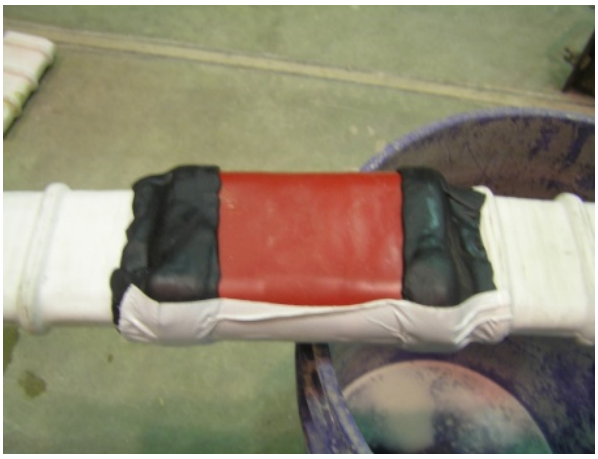

b. Butyl rubber and duct tape

Figure 3.2. Mockup splice connections for 1 in. x 3 in. P-T duct

3.3. Evaluation of the Influence of Surface Treatment on Transverse Joint

The precast panels require the transverse edges of the panels be “roughed” for shear resistance prior to grouting the transverse joints between each panel. Four different alternatives were tested to determine the most effective surface treatment for shear resistance; Control (i.e. no roughening), Diamond Plate Form, Chemical Etching, and Sandblasting. For each alternative, three specimens were tested, each specimen consisting of a 6 in. x 6 in. x 6 in. grout cube sandwiched between two concrete cubes of similar dimensions. Push-out tests for each specimen were performed on a SATEC 400HVL universal testing machine. No horizontal clamping force was used during the testing, therefore only the bond strength of the grout to the concrete cubes was tested.

The following four surface "roughening" alternatives were tested and evaluated: Control (i.e. no roughening), Diamond Plate forms, Chemical Etching, and Sandblasting. For each alternative, three specimens were tested, each specimen consisting of a 6 in. x 6 in. x 6 in. grout cube sandwiched between two concrete cubes of similar dimensions. Push-out tests were performed on each of the specimen as shown in Figure 3.3. Figure 3.4 illustrates a typical deflection vs. load curve for the sandblasted specimen. A progression in higher shear bond strength is evident as one move from the Control specimens, to Diamond Plate specimens, to Chemically Etched specimens, to Sandblasted specimens. Sandblasting appears to be the most effective surface treatment for resistance to pure shear.

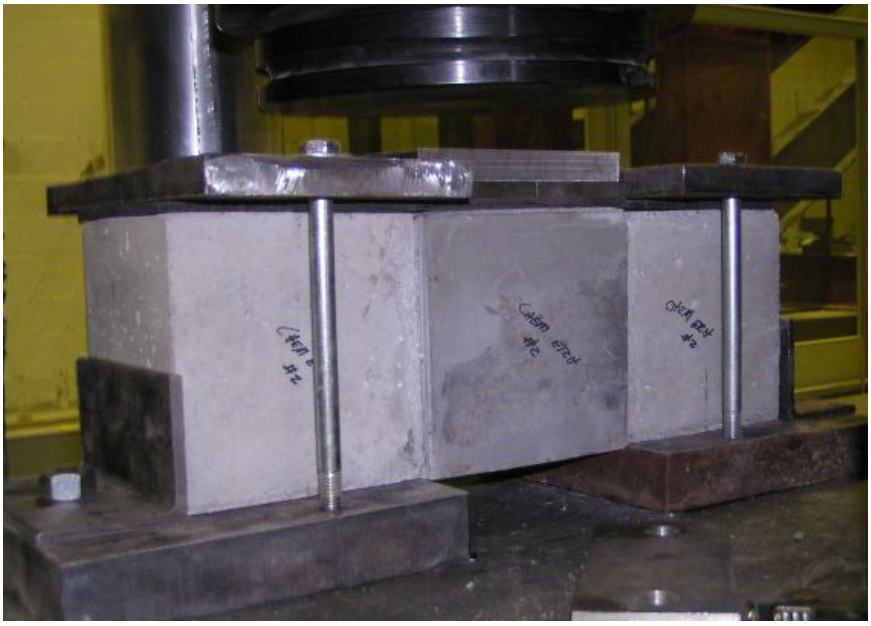

Figure 3.3. Push-out tests for transverse joint surface treatment

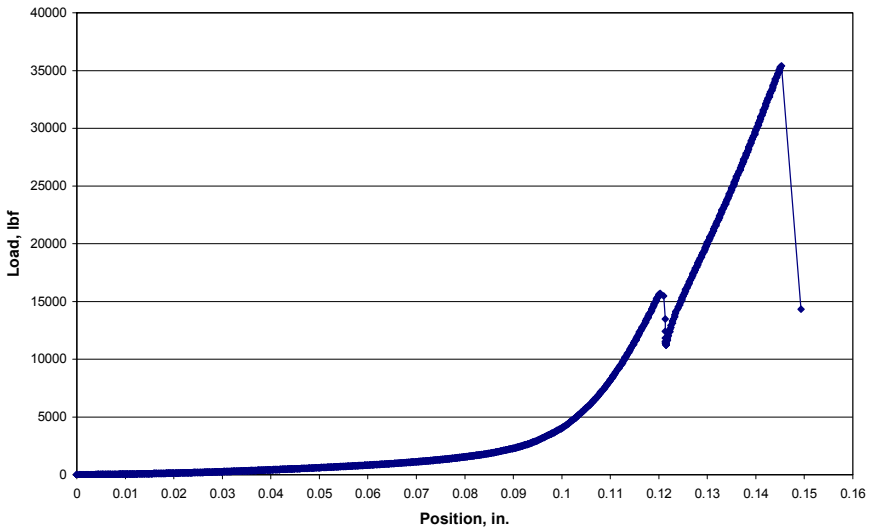

Figure 3.4. Deflection vs. Load plot for sandblasted specimen #3

3.4. Lab Testing Key Findings

Three laboratory tests were conducted to evaluate design and construction issues for the 24th Street Bridge in Council Bluffs, Ia. The tests consisted of evaluating the shear stud pockets, (including the stud bend test and grout flowability), evaluation of duct splicing performance, and the influence of surface treatment on transverse joint shear transfer. The following conclusions were made from the laboratory testing:

1. No difficulty in installing the shear studs in the precast panel pockets were foreseen by the contractor or encountered by the research team.
2. Conducting the bend test on the studs in the precast panel pockets was feasible for all six studs.
3. Grout with the proposed slump can sufficiently flow through the stud pockets into the haunch areas. It is anticipated that air will remain entrapped in these areas. The impact of the voids is not known.
4. The waterproof duct tape and butyl rubber methods of grout proofing the duct splices were both acceptable.
5. Sandblasting the surface of the concrete/grout joint was the most effective surface treatment for resistance to shear.

4. FIELD TESTING

Four field tests were performed in order to better understand the performance of the bridge components and the completed bridge. The first test consisted of corrosion monitoring both the prestress and post-tensioned strands within the precast deck panels. The monitoring took place during construction and shortly after construction was completed. Next, to better understand the impact that handling and placement has on the deck panels, two panels were monitored for strain behavior during placement. After the deck panels were placed and post-tensioning strands threaded, the joint stress between two adjacent panels was monitored during the tensioning and grouting of the strands. Lastly, a load test was performed monitoring deflection and strain of critical members.

4.1. Strand Corrosion Monitoring

Corrosion monitoring of the strands was completed with the use of Vetek V2000 corrosion monitoring system. Six transverse prestressed strands were instrumented with the corrosion monitoring systems during panel fabrication as shown in Figure 4.1. The post-tensioning strands were also monitored by placing three non-stressed sacrificial ducts with strands in two conjoining end panels. The actual strand could not be monitored due to the congestion within the post-tensioning duct. The locations of the strands in the bridge deck are shown in Figure 4.2. The V2000 monitor works by measuring the electric potential between the strand and the electrode with the pore water of the concrete acting as an electrolyte between the two. An increase in the electric potential indicates that corrosion activity is taking place. The electric potential is measured with a voltmeter with three different ranges of readings representing three different stages of corrosion. The three different stages are listed in Table 4.1.

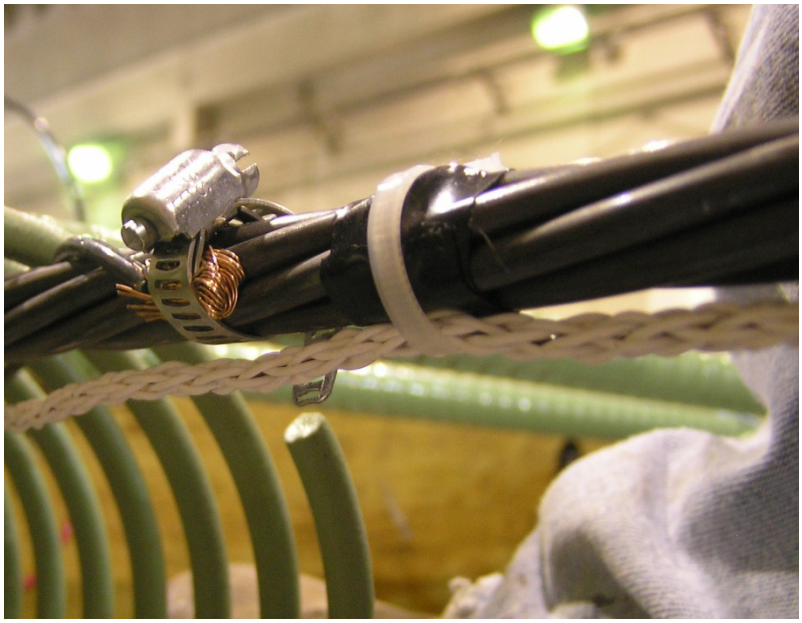

Figure 4.1. Corrosion electrode tied to strand

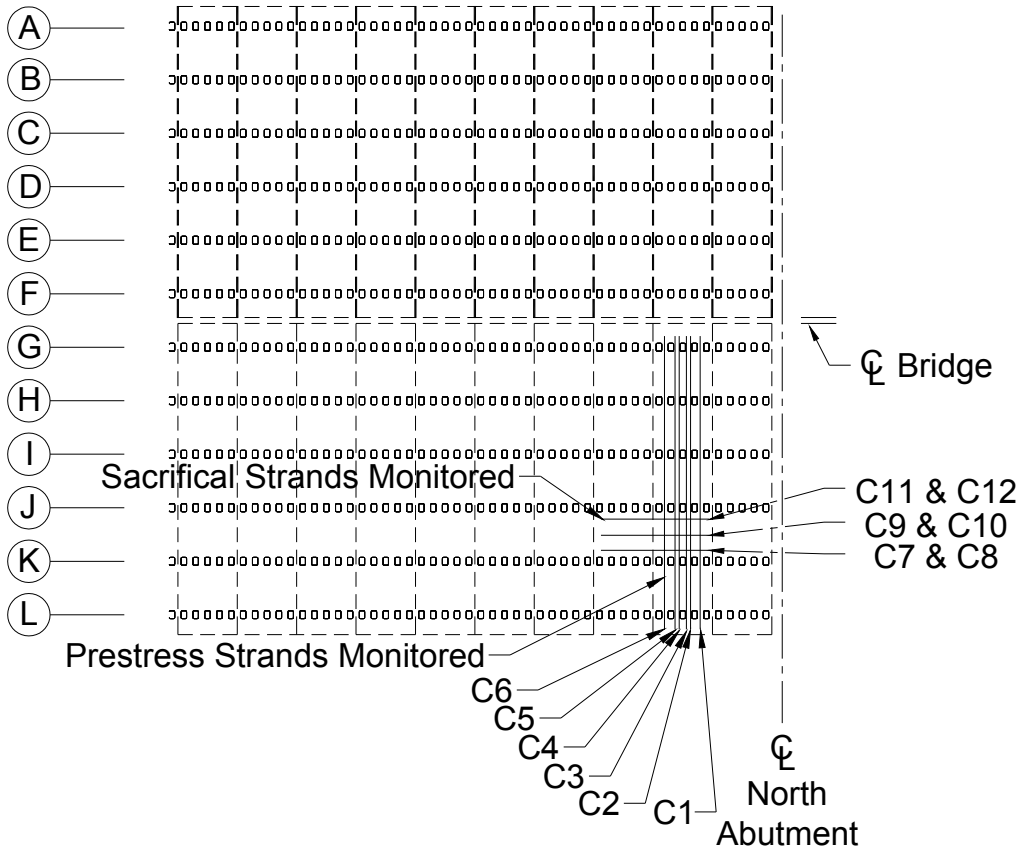

Figure 4.2. Location of strands monitored for corrosion at north abutment

Table 4.1. Vetek V2000 electrode readings

Range	Voltmeter Reading	Range Description
Range 1	Less than 300mV dc	No corrosion activity is taking place
Range 2	From 300mV to 400mV dc	Corrosion is either just starting or just stopping due to lack of oxygen
Range 3	400mV dc and above	Corrosion is fully active on the steel strand

Both the prestress and post-tensioning strands that were selected for monitoring were instrumented their full length. Electrode readings for the prestress strands were taken during the placement of the deck in 2008. The sacrificial post-tensioning strands were read after their placement in 2008. Both strands were again read in 2009. The results of the electrode readings are shown in Table 4.2. All electrode readings are within Range 1, indicating that no corrosion is taking place in the strands.

Table 4.2. V2000 millivolt electrode readings

Electrode Location	Date Tested (mV dc)		
	9.16.08	11.12.08	5.20.09
C1	40.4	n/a	0
C2	55	n/a	73.6
C3	62.4	n/a	0
C4	42	n/a	0
C5	294.4	n/a	93.4
C6	68.3	n/a	63.8
C7	n/a	266.3	211.9
C8	n/a	264.9	210.9
C9	n/a	259	230.1
C10	n/a	74.9	138.8
C11	n/a	-26.7	2.1
C12	n/a	263	216.2

*Readings in Range 2

**Reading in Range 3

4.2. Deck Panel Behavior during Handling

In order to better understand the behavior of the deck panels, two deck panels were monitored during their placement in the field. Each of the two deck panels were instrumented with 16 BDI strain gauges. The strain gauges locations and labels are shown in Figure 4.3. The deck panels were instrumented in the staging yard at the construction site, shown in Figure 4.4. Then the panels were lifted using 8 pick points. The panels were lifted with a crane, shown in Figure 4.5, to the proper location on the bridge and manually maneuvered into place as shown in Figure 4.6. The monitored panels had final placement over the pier during the Phase II construction. Each panel took about 20 minutes (1200 seconds) to place. The strain gauges continuously record data during the 20 minutes.

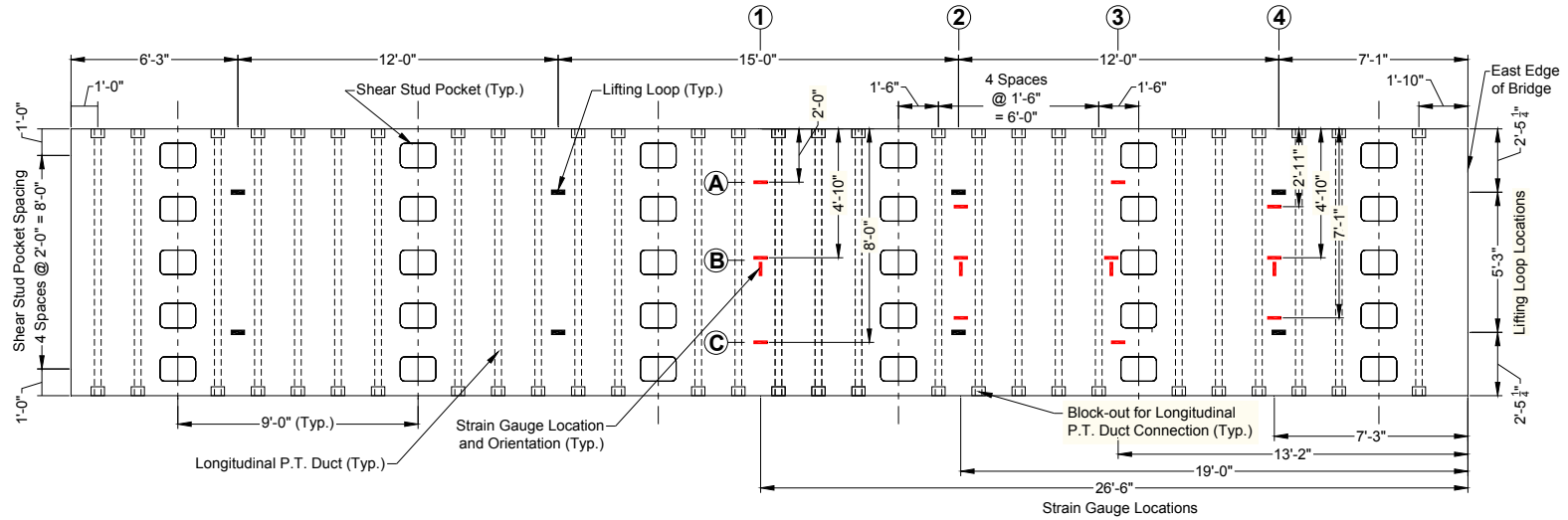

a. Panel No. 1

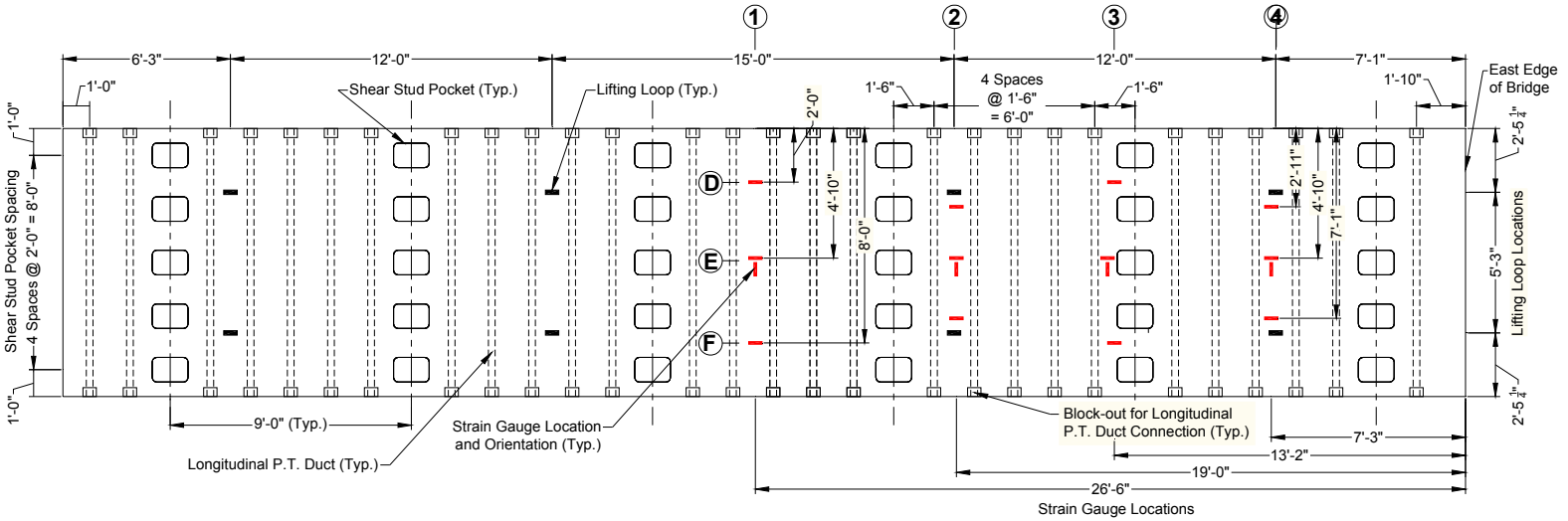

b. Panel No. 2

Figure 4.3. Strain gauge layout on precast deck panels

Figure 4.4. Precast deck panel in construction staging yard ready for placement

Figure 4.5. Deck panel being lifted into place

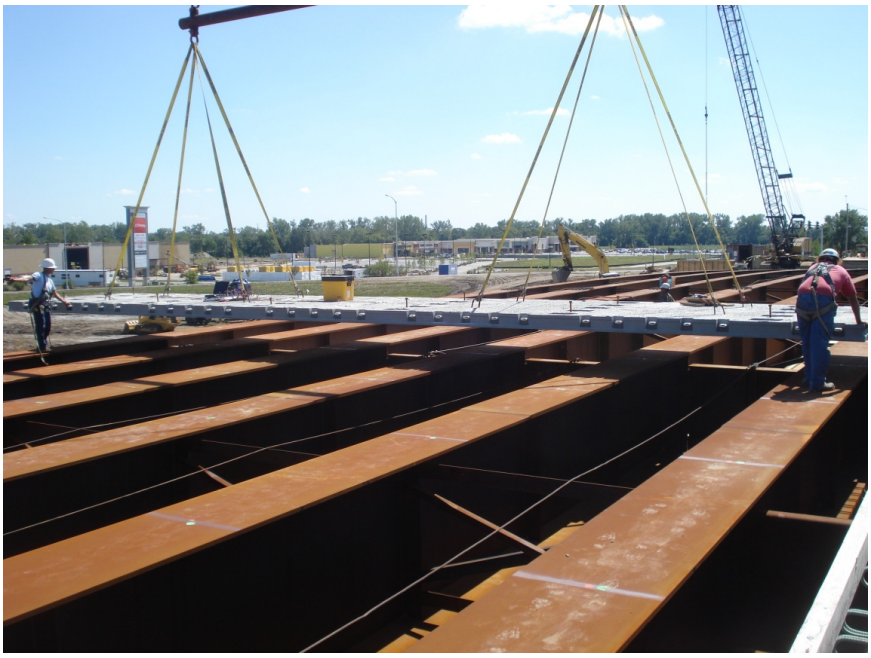

Figure 4.6. Final maneuvering of precast deck panel placement

The strain gauges were placed on top of the deck panels, as shown in Figure 4.3. The gauges locations are made of three alphabetical grid lines spaced longitudinally to the direction of traffic and 4 numeric grid lines space transversely to the direction of traffic. Only half of the transverse length of the panels was instrumented. The strain gauges are oriented on the deck panels with 12 of the gauges transverse to the directions of traffic and 4 longitudinal to the direction of traffic; these are denoted with an "L" after the gauge number. Figure 4.7 shows the strain gauges attached to the deck panel along a numeric grid line. Grid lines 2 and 4 are pick point locations for picking up and moving the panels.

Figure 4.7. Strain gauge orientation for each gauge line

The strain results for Panel No 1 are shown in Figure 4.8. As shown by the strain, the panel was fully lifted after 40 secs., representing the spike in the strain reading. Then, as the crane lifted and swung the panel over to the bridge, the strain peaked (68 με) at about 240 secs. At approximately 550 secs. to 1250 secs., the construction workers were aligning the panel to the proper location on the girders. At some points during this time the panel had points of contact with the girders.

After 1250 secs., the panel was in place and had its leveling bolts resting completely on the girders. The transverse strain along grid line 1, which is the center line of the panel, showed the highest strain readings. The strain on grid line 1 varied from 55 με to 68 με all in tension. The longitudinal gauges located along gridline B varied between 3 με to 40 με all in compression during the placement of the panel.

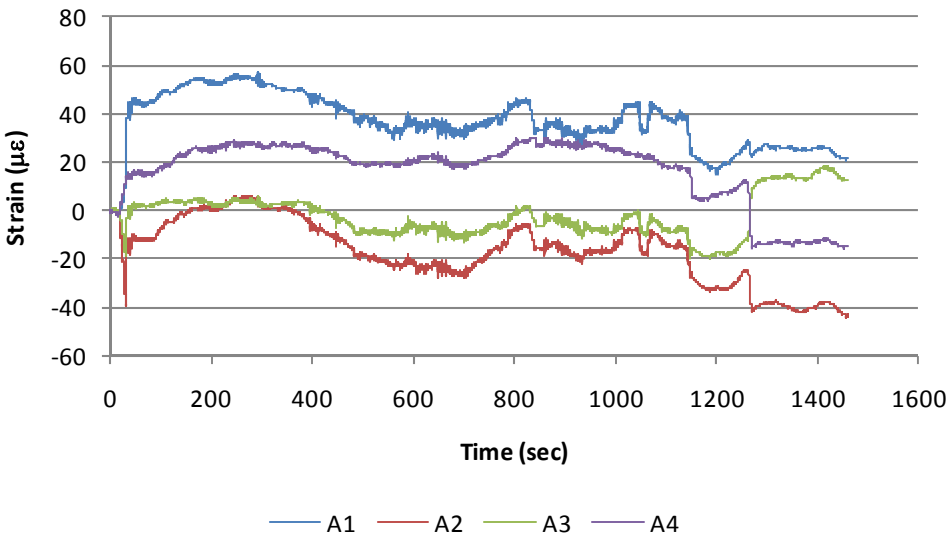

a. A-line strain readings

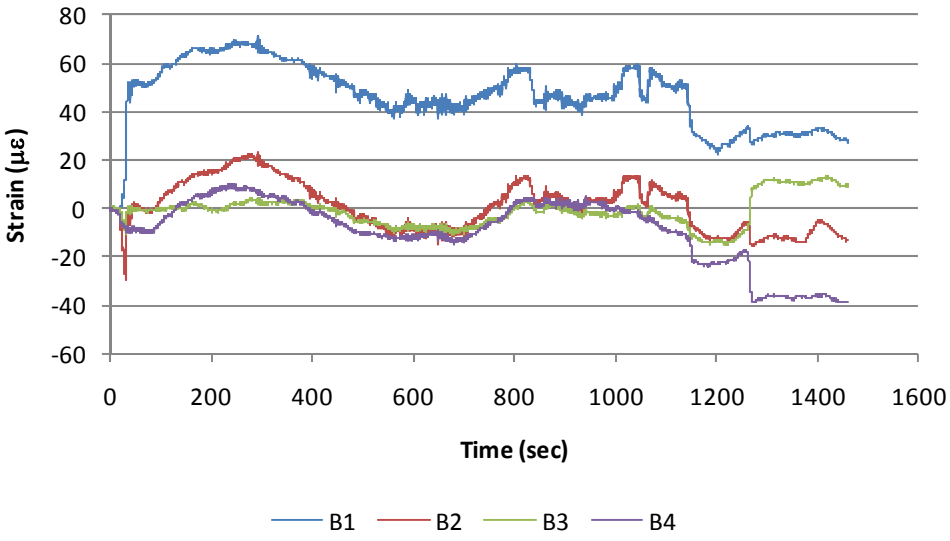

b. B-line strain readings

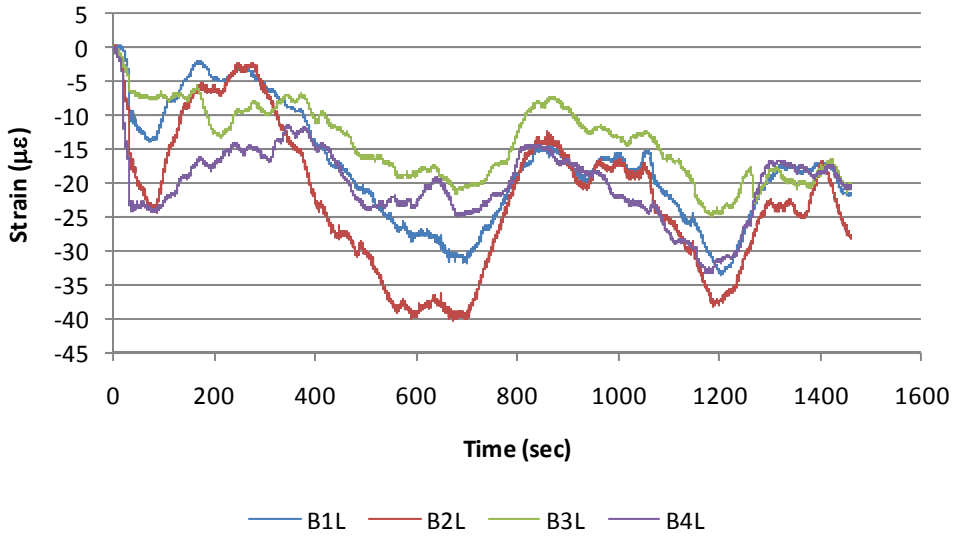

c. B-line longitudinal strain readings

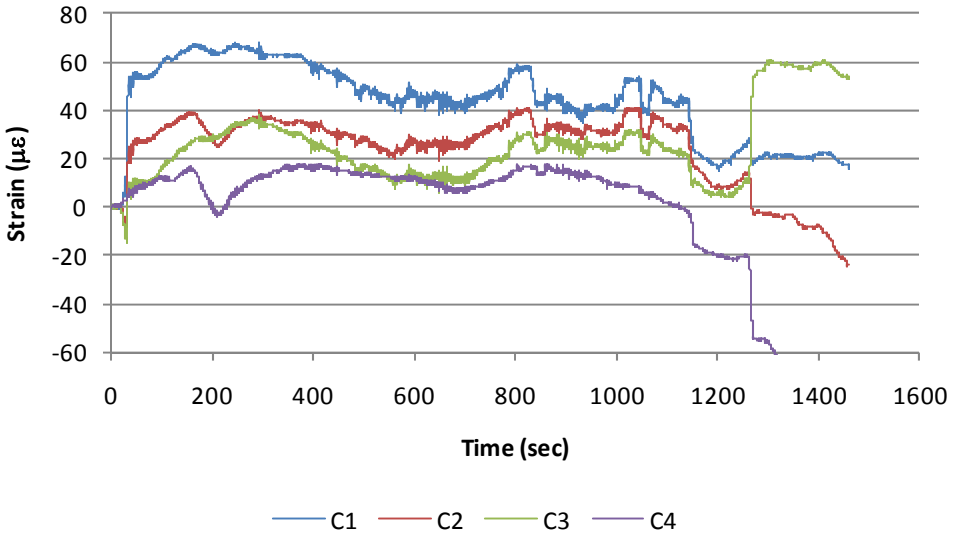

d. C-line strain readings

Figure 4.8. Panel No. 1 strain readings during panel placement

Figure 4.9. shows the strain profile along grid lines A, B, and C at time 33 secs. and 240 secs. At 33 secs., the panel is fully picked up and at 240 secs., the panel reaches its maximum strain at nearly all the strain locations. At location zero, which is grid line 1 and center line of the panel,

the strain is at its maximum. In general, the strain decreases as it moves away from the center of the panels. The strain at and between the pick points have very little consistency between gridlines.

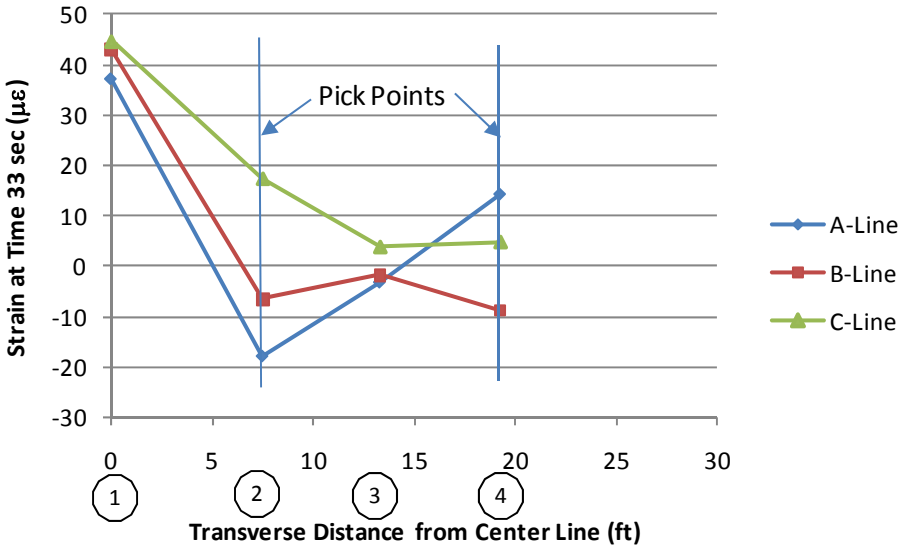

a. Strain at 33 seconds

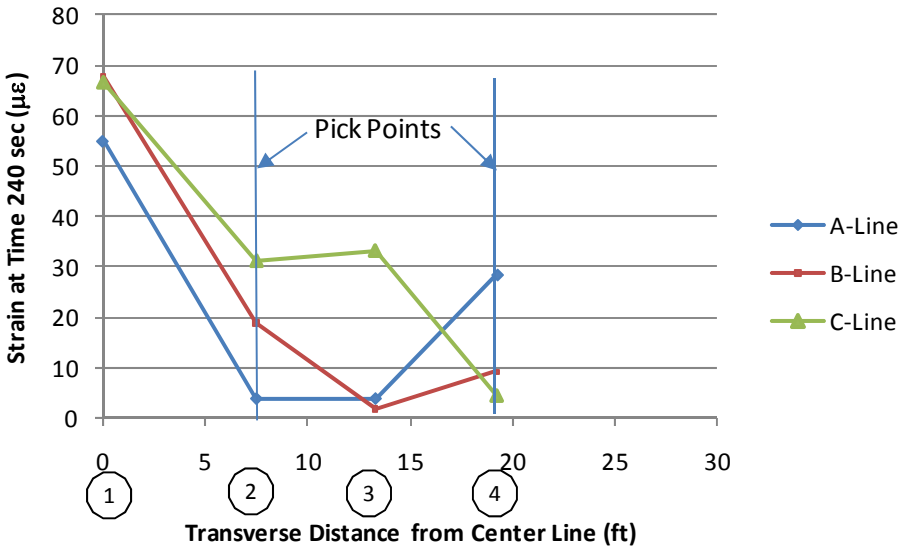

b. Strain at 240 seconds

Figure 4.9. Strain profile along gridlines A, B, and C, Panel No. 1

The strain readings for Panel No. 2 are shown in Figure 4.10. As seen at approximately 63 secs. the panel is fully picked up. The panel was then lifted and swung over the girders. At approximately 560 secs., the panel was being maneuvered by the construction workers into placement. Then, at approximately 1150 secs., the panel's leveling bolts were fully resting on the girders. Panel No. 2 reached a maximum strain of approximately 230 με. The maximum strain occurred at location F2. At the time of maximum strain the strain in all the gauges varied from 48 με to 230 με. The lowest strain consistently occurred along gridline 4.

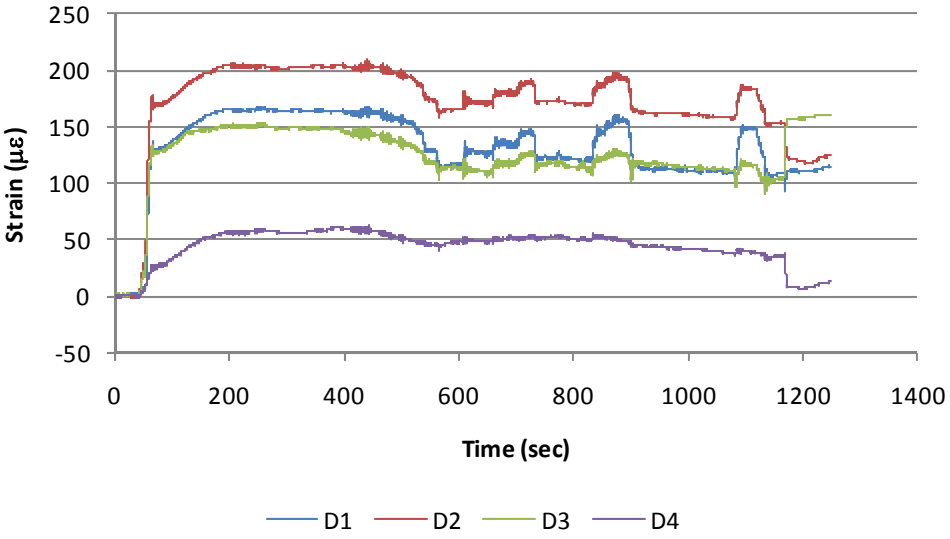

a. D-line strain readings

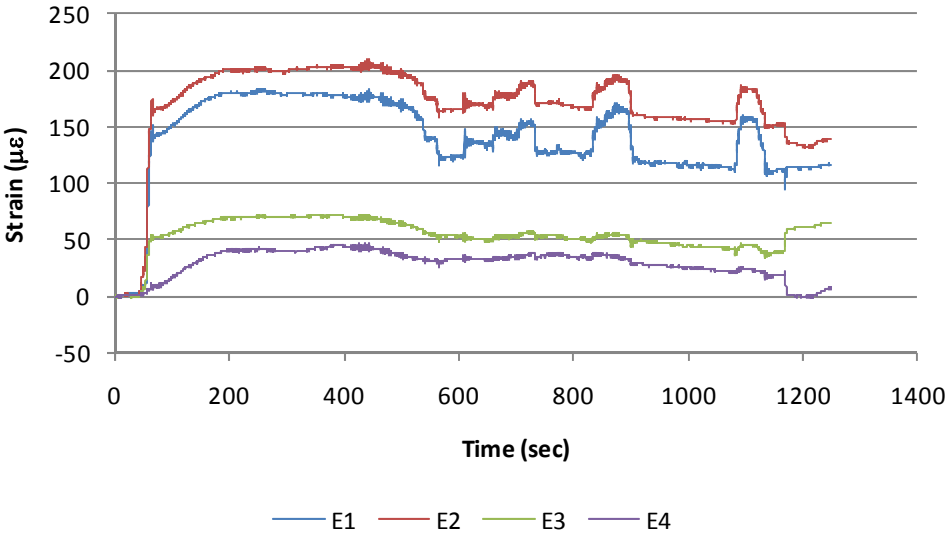

b. E-line strain readings

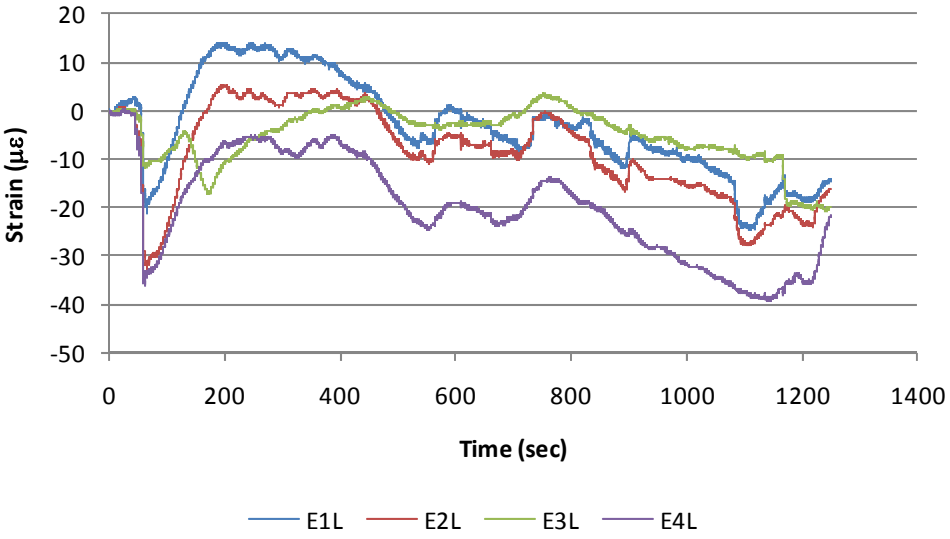

c. E-line longitudinal strain readings

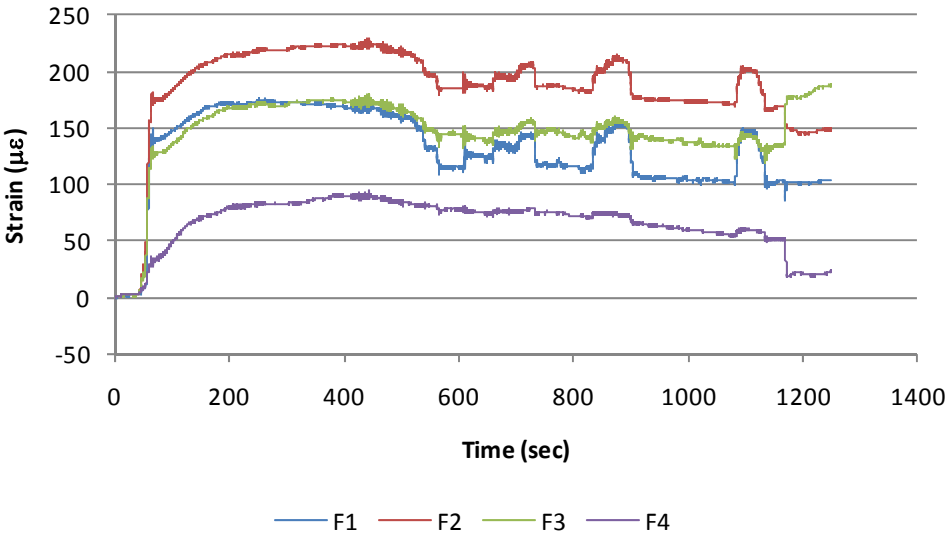

d. F-line strain readings

Figure 4.10. Panel No. 2 strain readings during placement

The strain profile along grid lines D, E, and F are shown in Figure 4.11 at time 63 secs. and 441 secs. At time 63 secs., (time at which panel is full picked up) the strain at gridline 1 (centerline of the panel) is at approximately 130 με. The strain then increases to the pick point at gridline 2 to 160 με. The strain then steadily decreases to gridlines 3 and 4. The strain at gridline 4 is approximately 30 με. A similar pattern occurred at time 441 secs. (time at which panel reach max strain); however, the strain values were higher. At gridline 1 the strain was approximately 170 με□, then it increased to approximately 210 με and then went down to an average value of approximately 70 με at gridline 4.

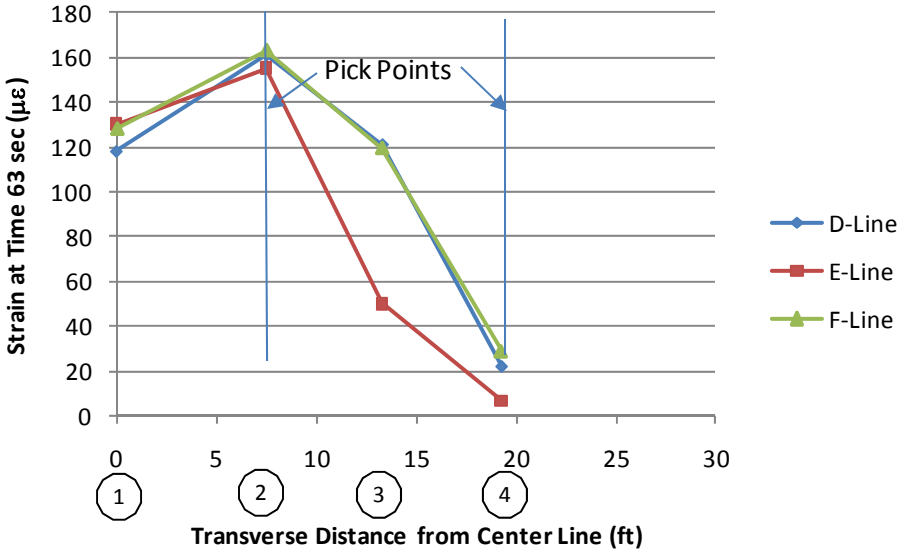

a. Strain at 63 seconds

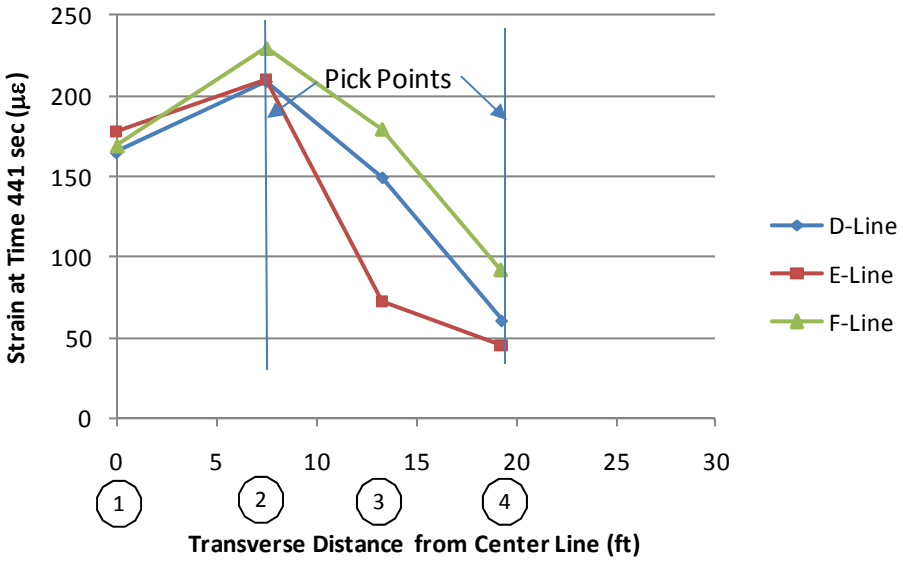

b. Strain at 441 seconds

Figure 4.11. Strain profile along gridlines D, E, and F, Panel No. 2

4.3. Post-tensioning Strand Behavior during Stressing

Load cells were placed in the precast deck panel joints prior to grouting in order to determine post-tensioning pressures in the slab. Six load cells were placed in the panel transverse joint located 4 ft south of the centerline of the pier during Phase II constructions. Three load cells each were located between girder I and J and J and K. Figure 4.12 illustrates the location of the load

cells in the panel. The final installation of the load cells is shown in Figure 4.13. A bolt was used at the contact point for the load cell. Prior to grouting the bolt was screwed out to make firm contact with the load cell. The contact between the load cell button and bolt head was sealed with silicon to eliminate grout infiltrating the contact point.

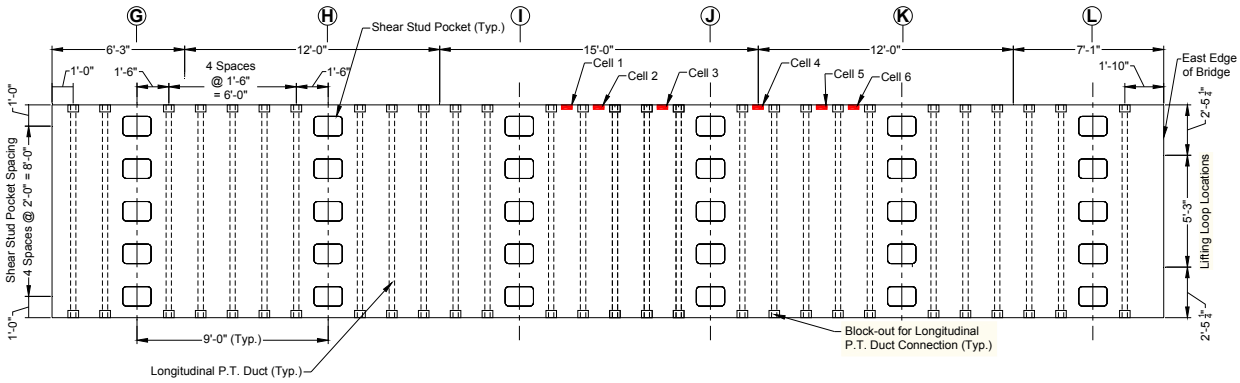

Figure 4.12. Location of load cells in precast deck panels

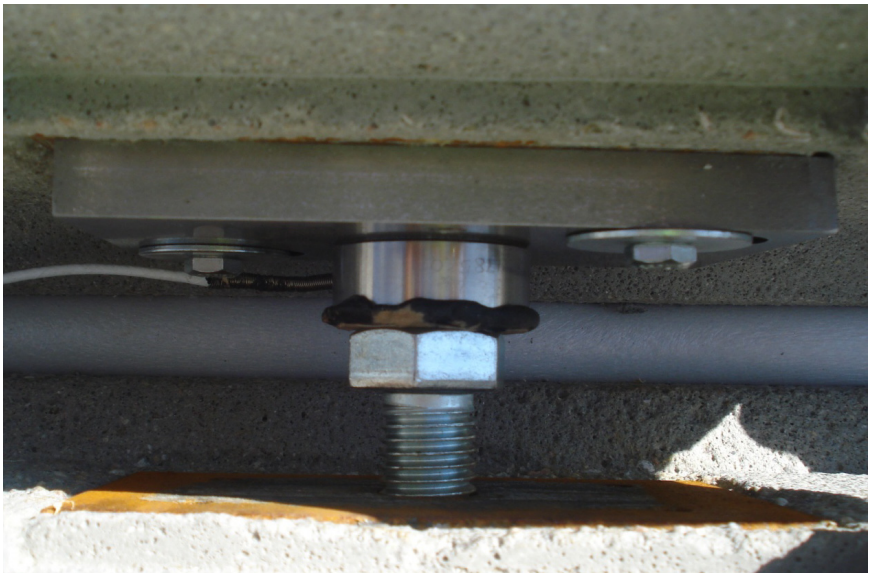

Figure 4.13. Final installation of load cell in deck joint (top view)

As the deck was post-tensioned from both the south and the north ends, load cell readings were taken continuously. The post-tensioning process took approximately 12 hours total and each strand was elongated approximately 21 to 22 in. The stress at each load cell during the 12 hours of recording is shown in Figure 4.14. The maximum stress obtained from the load cells was from Cell 2, which had a maximum stress of approximately 950 psi. Due to the negative pressure readings and non-uniform stress from load cell to load cell, it is uncertain if all the load cells were working properly during post-tensioning. Load Cell 6 did not record data during the post-tensioning.

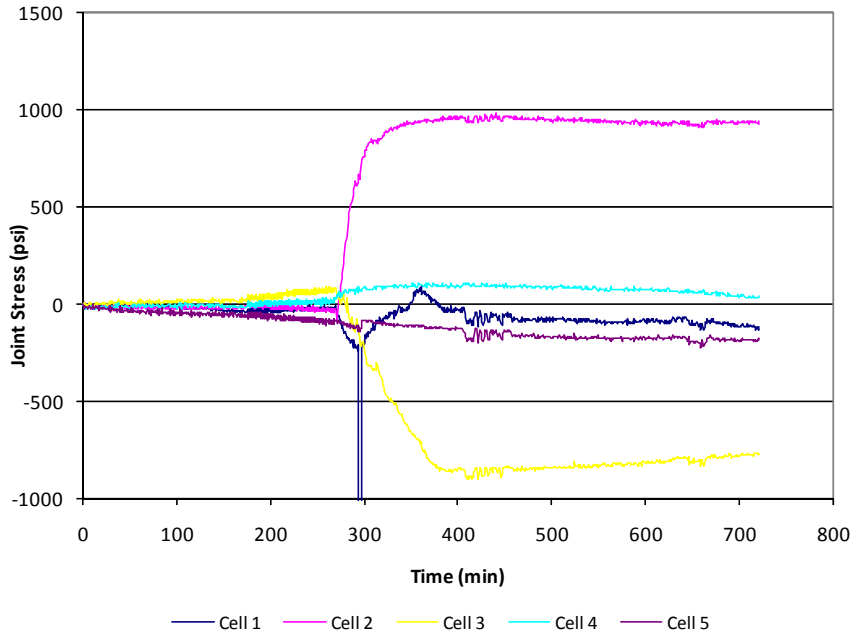

Figure 4.14. Deck panel load during strand stressing

4.4. Diagnostic Live Load Testing

A diagnostic live load test was conducted on the completed bridge to compare structural performance with expected design performance. Strain gauges and deflection transducers were installed on critical superstructure members. BDI strain gauges were placed at the pier, mid-span, and abutment of the north span as shown in Figure 4.14. The gauges had three different configurations as depicted by the number next to the gauge location in Figure 4.14. The three different configurations are shown in Figure 4.15. Deflection transducers were placed on girders F through L at the mid-span of the north span only. The deflections transducers were placed on the bottom of the girder similar to configuration 1 in Figure 4.15. Accelerometers were also placed at mid-span and quarter-span of the bridge north span.

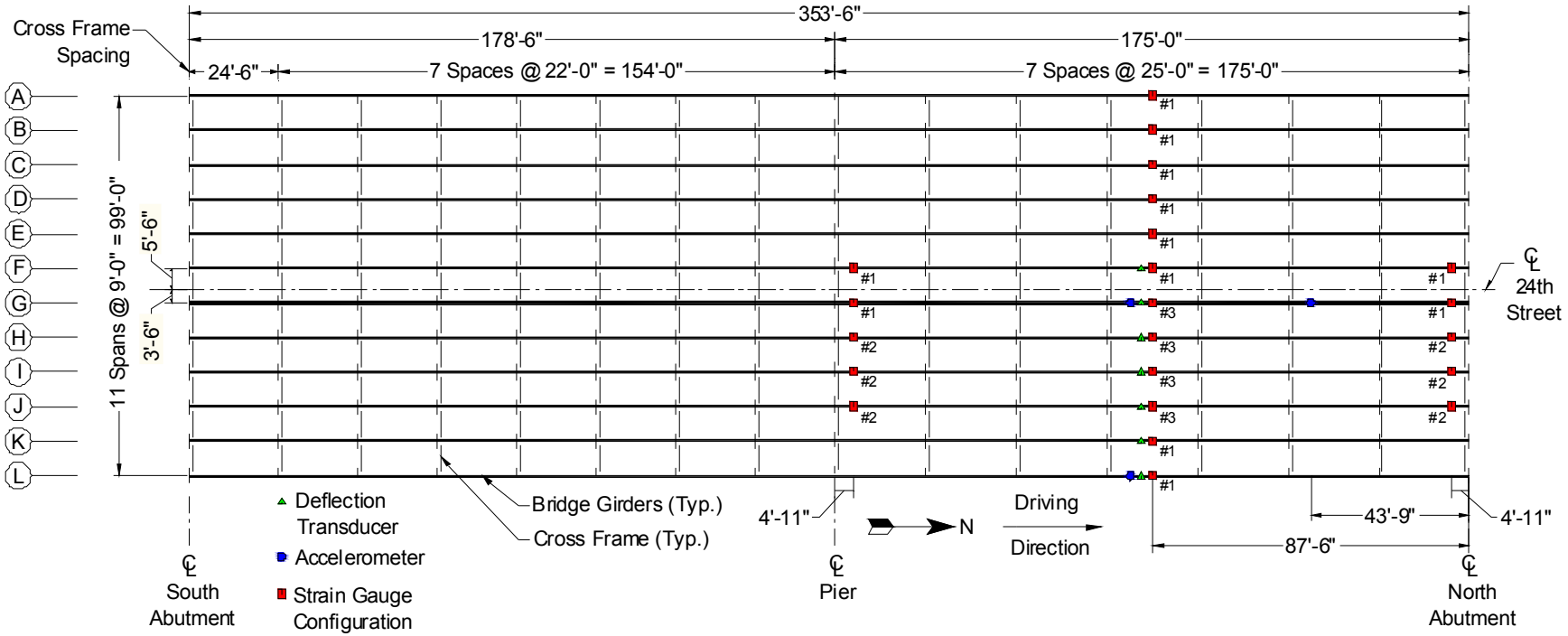

Figure 4.15. Gauge location on bridge

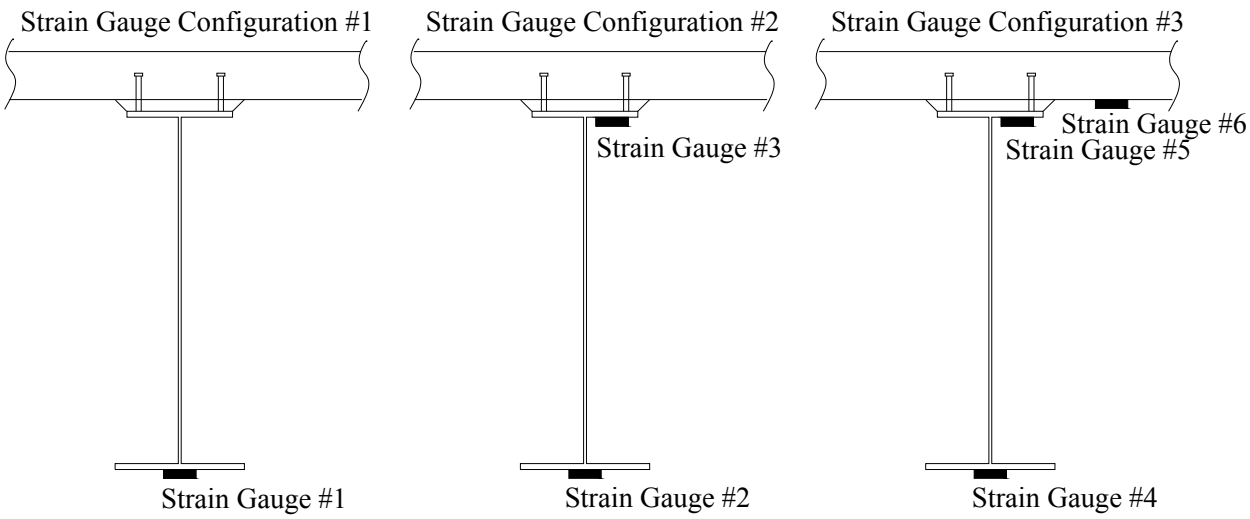

Figure 4.16. Cross-sectional strain gauge configurations

Field testing took place on November 12, 2008. The testing consisted of point-in-time live load testing with a fully loaded three axle dump truck that was driven over the bridge at slow speeds. The transverse position of the truck varied with six load cases (LC) 1 through LC 6, as shown in Figure 4.16. The loaded dump truck used for testing has a gross weight of 49 220 lb. The axle configurations and weights can be seen in Figure 4.17. The testing was conducted at night with only the loaded lane being closed to ambient traffic. Although tests were conducted when ambient traffic was low, there were load cases with heavy trucks driving over the bridge.

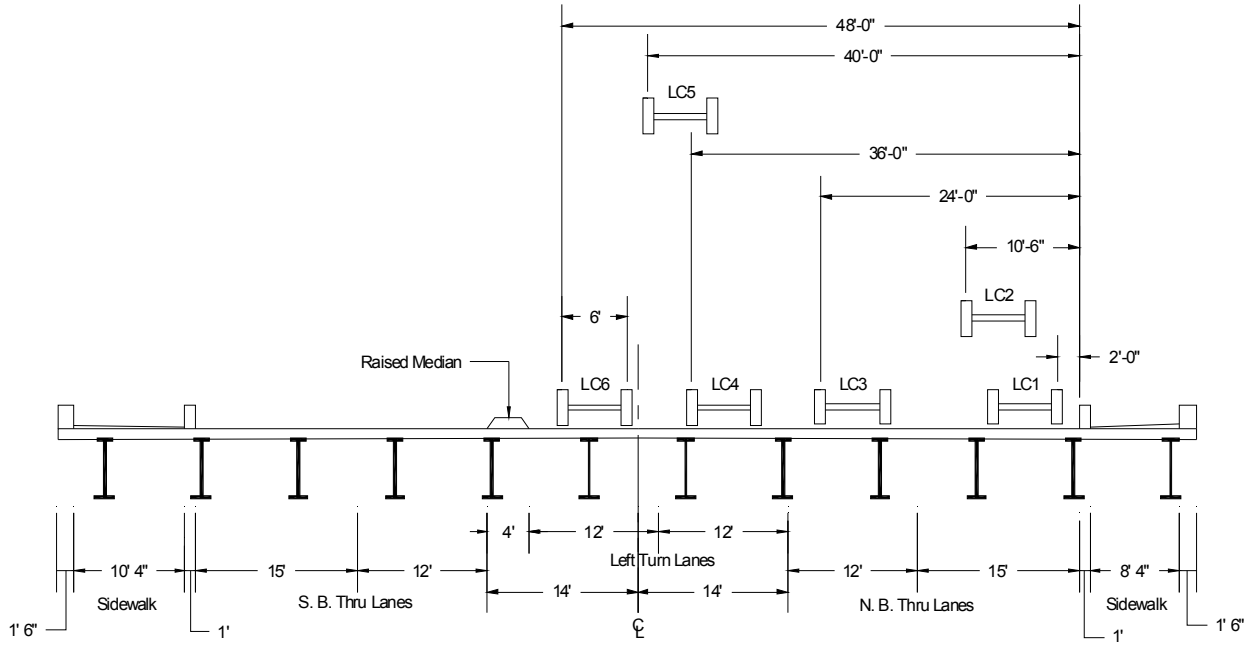

Figure 4.17. Truck load paths (truck traveled north into the page)

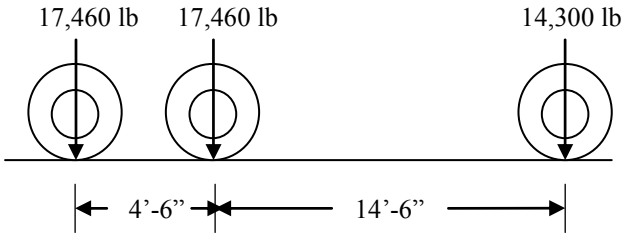

Figure 4.18. 2008 truck axle loads

4.4.1. Girder Deflection

Deflection transducers were installed on the bottom flange of the seven east girders. Representative time-history deflections for load case 2 at the north span mid-span with respect to front axle position are shown in Figure 4.18. The load truck was located in the center of the east driving lane for load case 2. In general all load cases produced the same deflection shape for the bridge with positive deflection when the truck was on the south span and negative deflection when the truck was on the north span. For all the load cases a deflection range of -0.32 in. to +0.21 in. was seen when the truck was on the south span and a range of -0.41 in. to +0.23 in. when the truck was on the north span for the seven girders. The maximum north span deflection of -0.41 in. corresponds to a span to deflection ratio of L/5120.

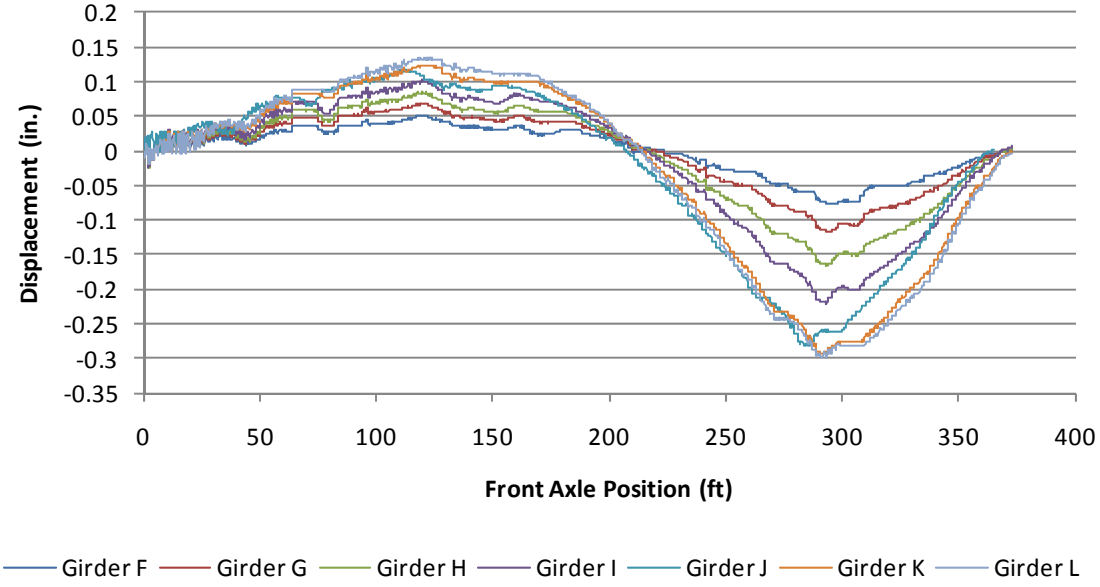

Figure 4.19. Representative time history deflections for Load Case 2

4.4.2. Girder Strain

A total of 36 strain gauges were placed on the bridge with 20 located at mid-span and 8 located at both the pier and north abutment. The cross-sectional strain gauge configurations are shown in Figure 4.15. Figure 4.19 through 4.21 represents the time history strain for the girder bottom flange location at the abutment, mid-span, and pier locations respectively. Figure 4.22 shows the strain at girder J having a strain gauge configuration of #3. The top flange strain and the strain on the bottom of the slab are very similar, indicating composite action between the girder and slab is taking place. The strains also indicate the natural axis is near the interface of the slab and girder. The full range of strain measured for all gauges can be seen in Table 4.3. The maximum strain was +66με and occurred at girder L during LC1. The largest strain range was at the mid-span-bottom flange location with a range of 88με during LC1.

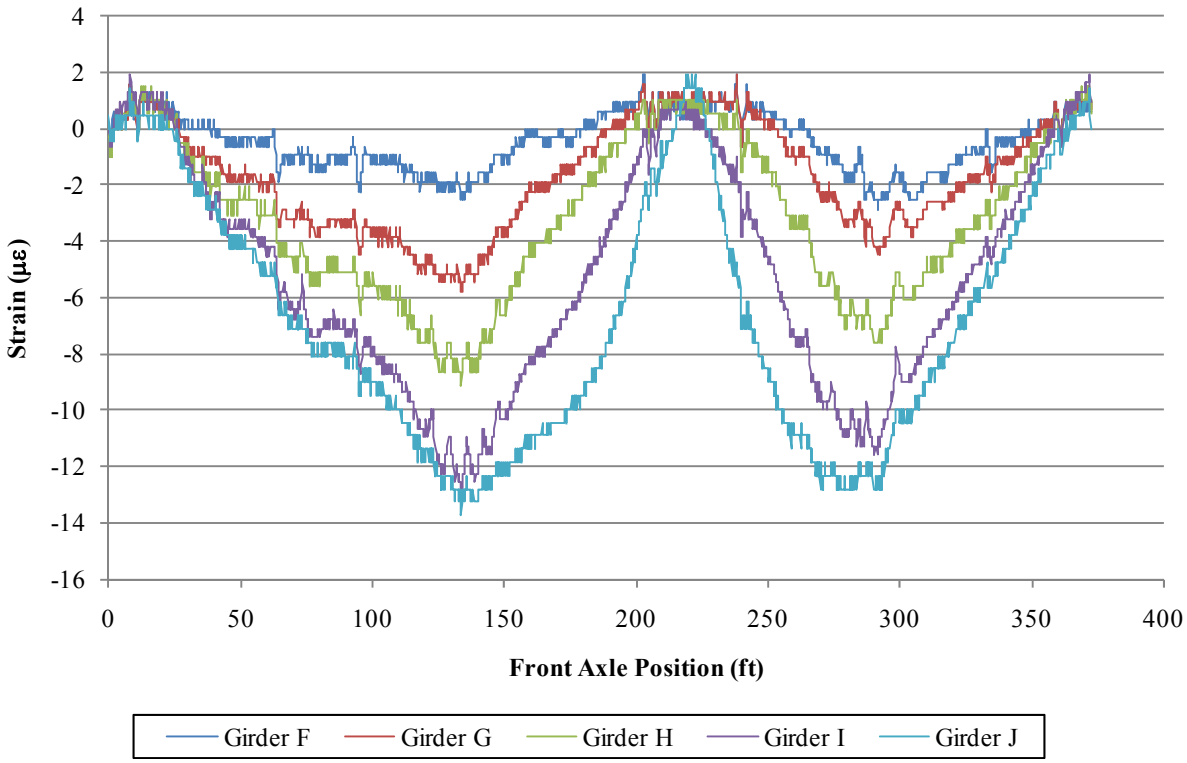

Figure 4.20. Representative time history strain at pier bottom flange load location, Load Case 2

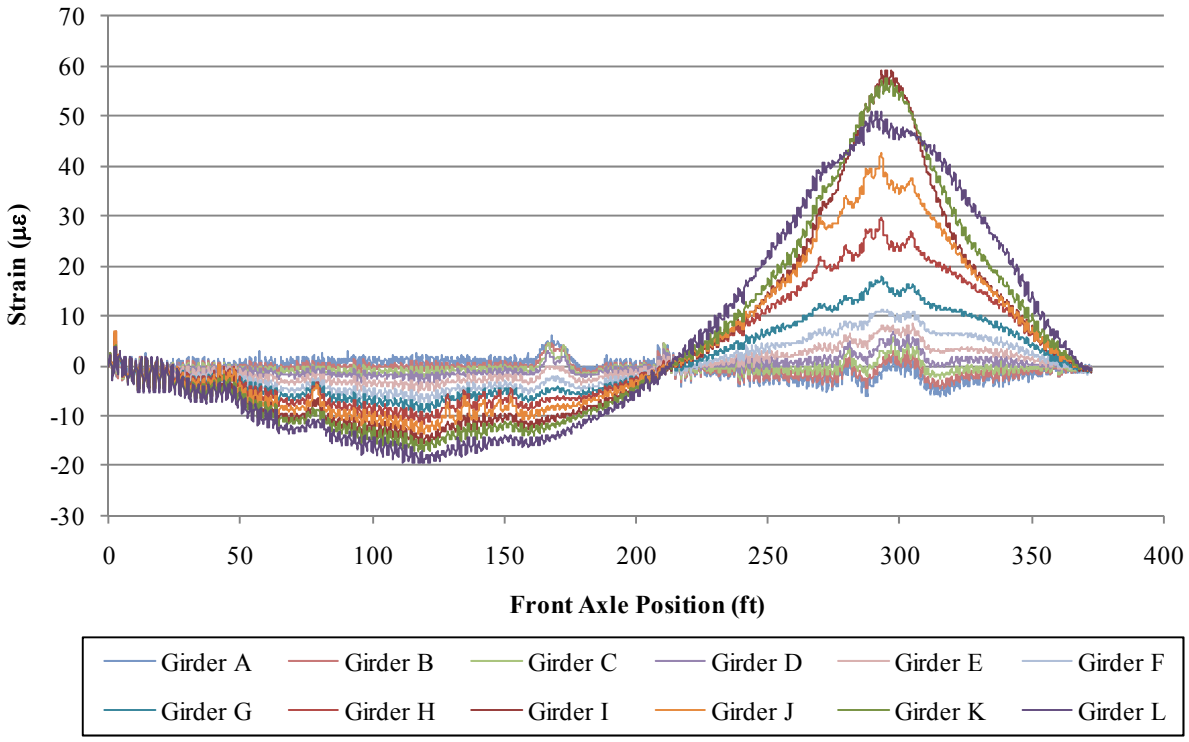

Figure 4.21. Representative time history strain at mid-span bottom flange load location, Load Case 2

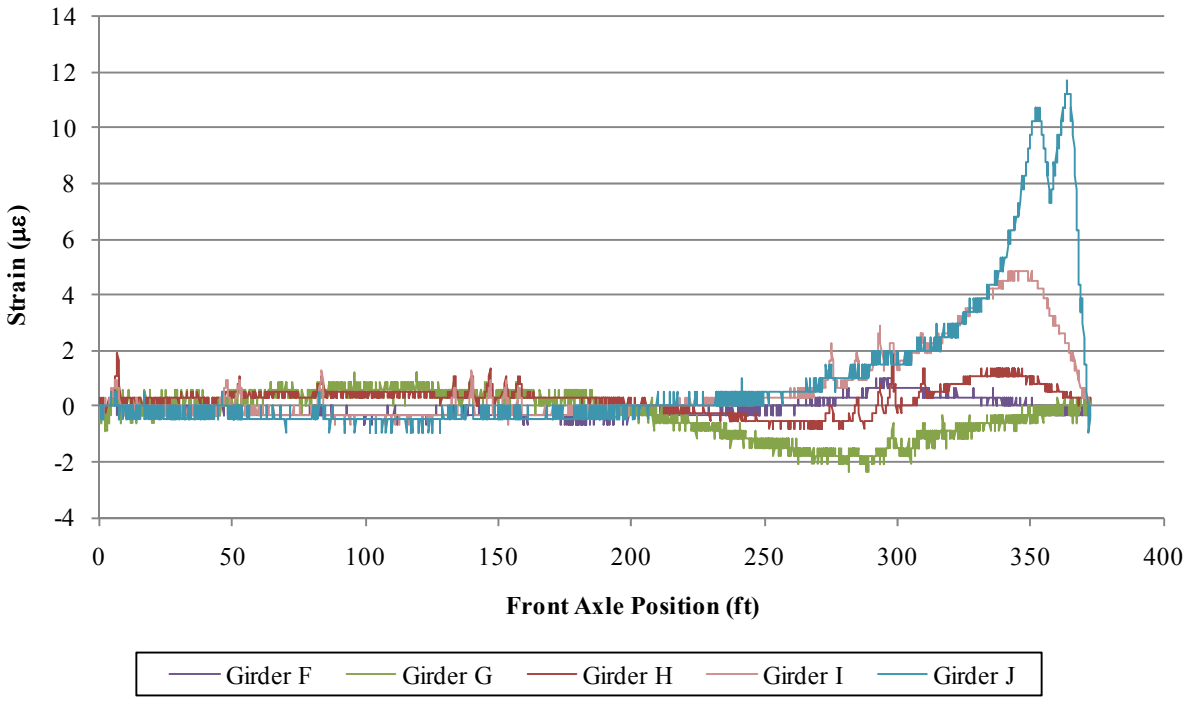

Figure 4.22. Representative time history strain at abutment bottom flange load location, Load Case 2

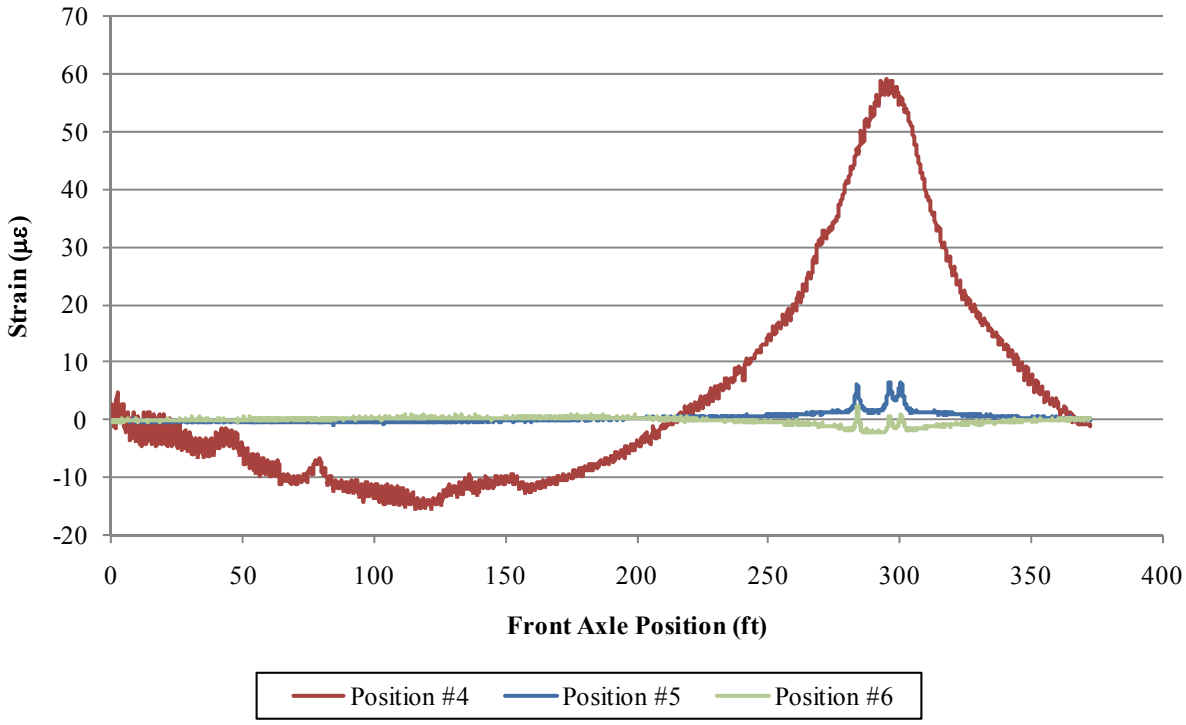

Figure 4.23. Girder J cross-section strain, Load Case 2

Table 4.3. Range of strain at various locations

Location	Strain (με)		
	Bottom Flange	Top Flange	Bottom of Slab
Abutment	-4 to +14	-5 to +6	NS
Pier	-16 to +3	-1 to + 5	NS
Mid-span	-22 to +66	-5 to + 5	-2 to + 6

NS—No strain gauge at location

4.4.3. Closure Pour Movement

The close pour movement is shown in Figure 4.23 and Figure 4.24 for LC5 and LC6 respectively. The deflections used to monitor the closure pour are located on the bottom of Girder F and G, which are on each side of the closure pour. The differential movement for both load cases was less than 0.04 in. The load distribution of the girders during the load test could cause some differential reading to occur; therefore, the actual movement at the joint would be less than the 0.04 in. shown in the figures.

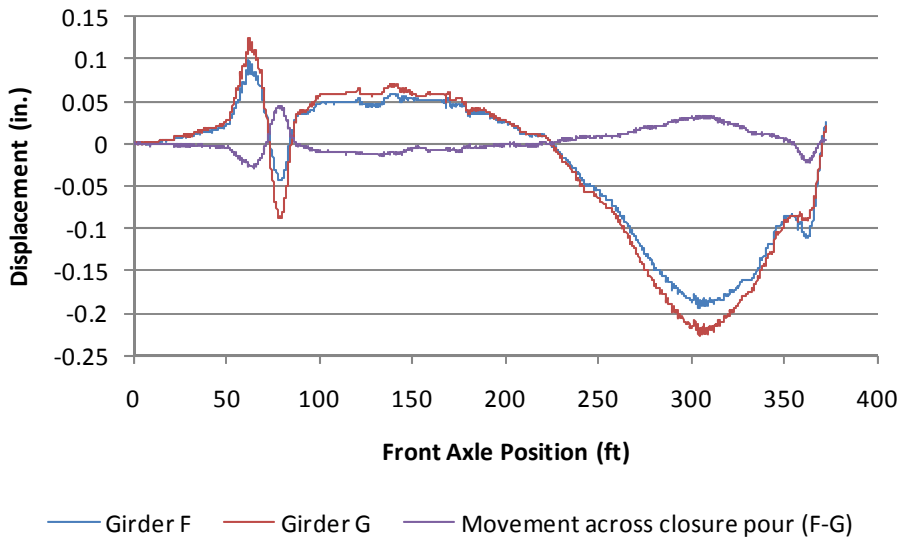

Figure 4.24. Load Case 5 girder deflection and differential movement at closure pour

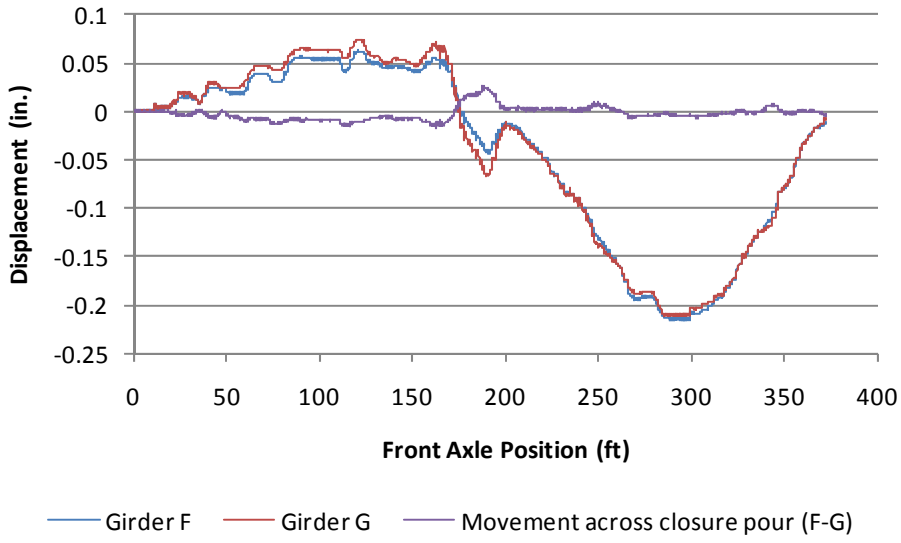

Figure 4.25. Load Case 6 girder deflection and differential movement at closure pour

4.4.4. Bridge Load Fraction and Load Distribution

Load fraction was calculated for each load case based on the assumption that the girders are of equal stiffness. The approximate load fraction for each girder can, therefore, be obtained with the following equation:

$$LF_i = \frac{\varepsilon_i}{\sum_{i=1}^{n} \varepsilon_i}$$

where LF_i = load fraction of the ith girder, ε_i = strain of the ith girder, $\Sigma\varepsilon_i$ = sum of all girder strain, and n = number of girders.

Figure 4.25 shows the load fraction for the six load cases tested. Girder K was seen to have the largest load fraction of 0.25 during LC 1. The girder with the lowest load fraction, near zero, was Girder A, which was furthest away for the load truck. The load fraction was generally largest at the girders directly below the truck. The load fraction generally decreased as the transverse distance from the girder to the load truck increased. During LC 5, however, the load fraction was affected by ambient traffic on the west side of the bridge, causing the load distribution to be near horizontal on the west side of the bridge.

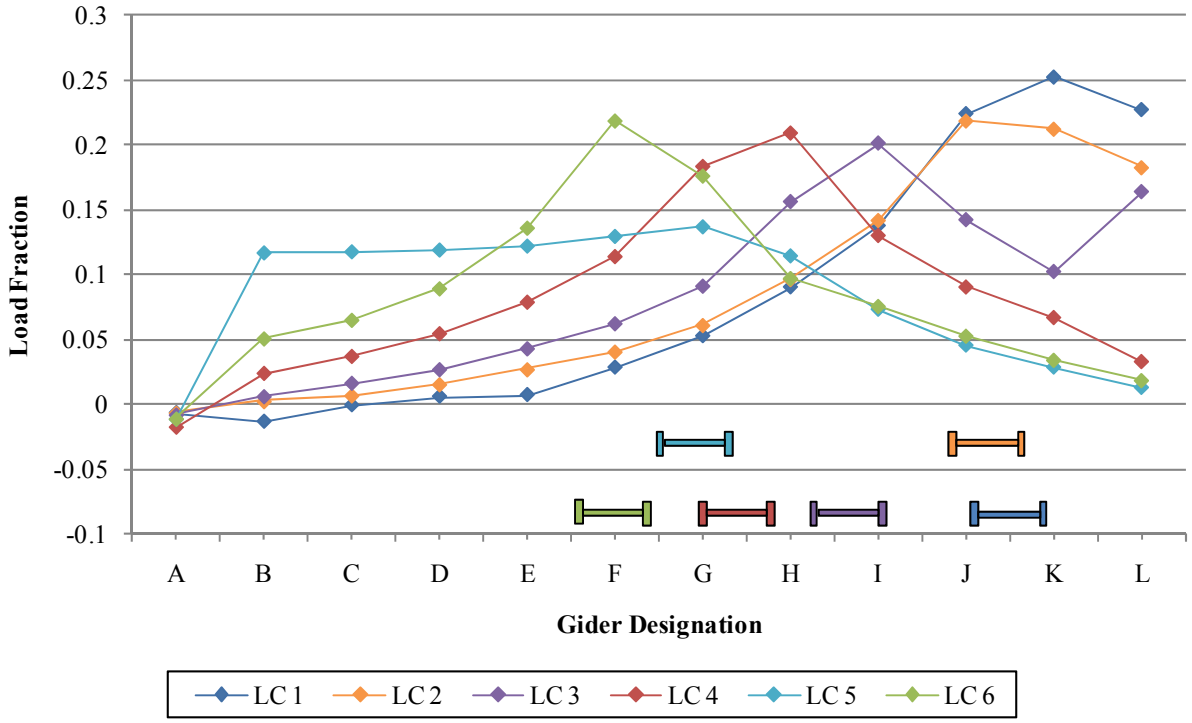

Figure 4.26. Experimentally-obtained load fraction for six load cases

Load distribution was determined experimentally by adding the load fractions of complementing load cases. Combining LC2, LC3, LC4, and LC6 with the transpose of LC2 and LC3 (designated at LC2' and LC3') provided proper lane loads for determining load distribution. Figure 4.26 shows the load fractions of the six load cases combined for load distribution. Figure 4.27. shows the experimental load distributions along with the code distribution factors from the American Association of State Highway and Transportation Officials (AASHTO) Load and Resistance Factor Design (LRFD) 2004. The largest obtained load distribution factor was obtained at Girder H with a value of 0.63. The lowest girder distribution factor was 0.30, which was located at Girder A. Girder A and L, however, are located below the side walk areas; therefore, Girder B and K may be more representative of the load distribution at the edge girders. The lowest distribution at Girder B and K was 0.42. When comparing the experimental test results with AASHTO LRFD load distributions, the experimental results were less than code distributions.

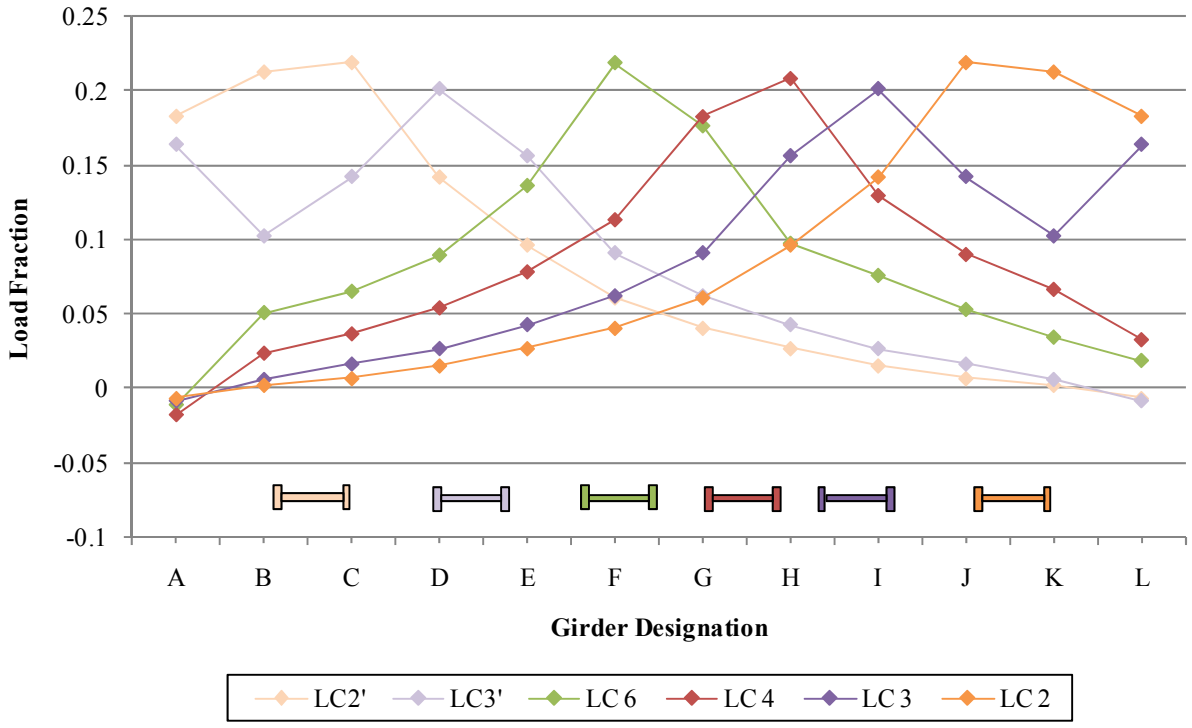

Figure 4.27. Load fractions combined to form load distribution

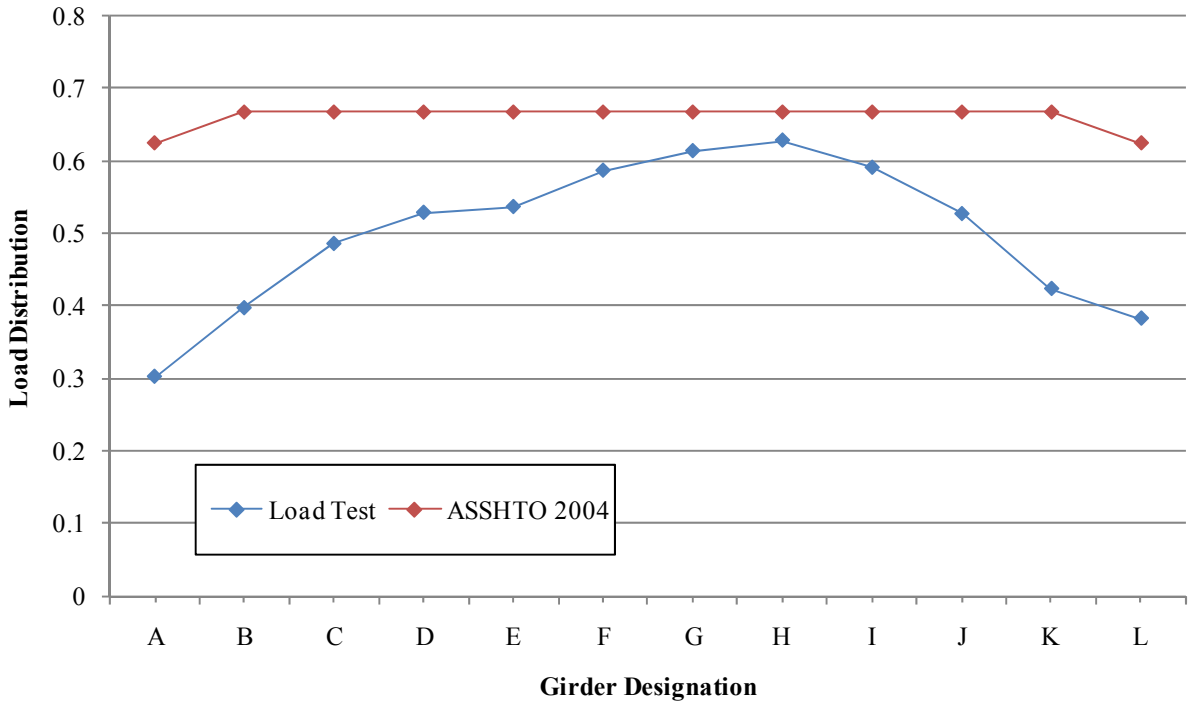

Figure 4.28. Experimental and codified load distributions

4.4.5. Evaluation of Neutral Axis Location

The girders with strain configuration #3 were used to estimate the location of the neutral axis during testing. Figure 4.28 and Figure 4.29 shows the strain profile for girder G through J for LC2 and LC3.The steel girder total depth was 61 in. with 1 in. flanges top and bottom. A girder haunch existed between the precast panel and girder of between ½ in. to 1 in. The location of the neutral axis during testing was approximately 58 in. to 61 in. from the bottom of the girder. The neutral axis location appears to be located near the top of the steel girder but not within the grouted haunch region or in the precast slab.

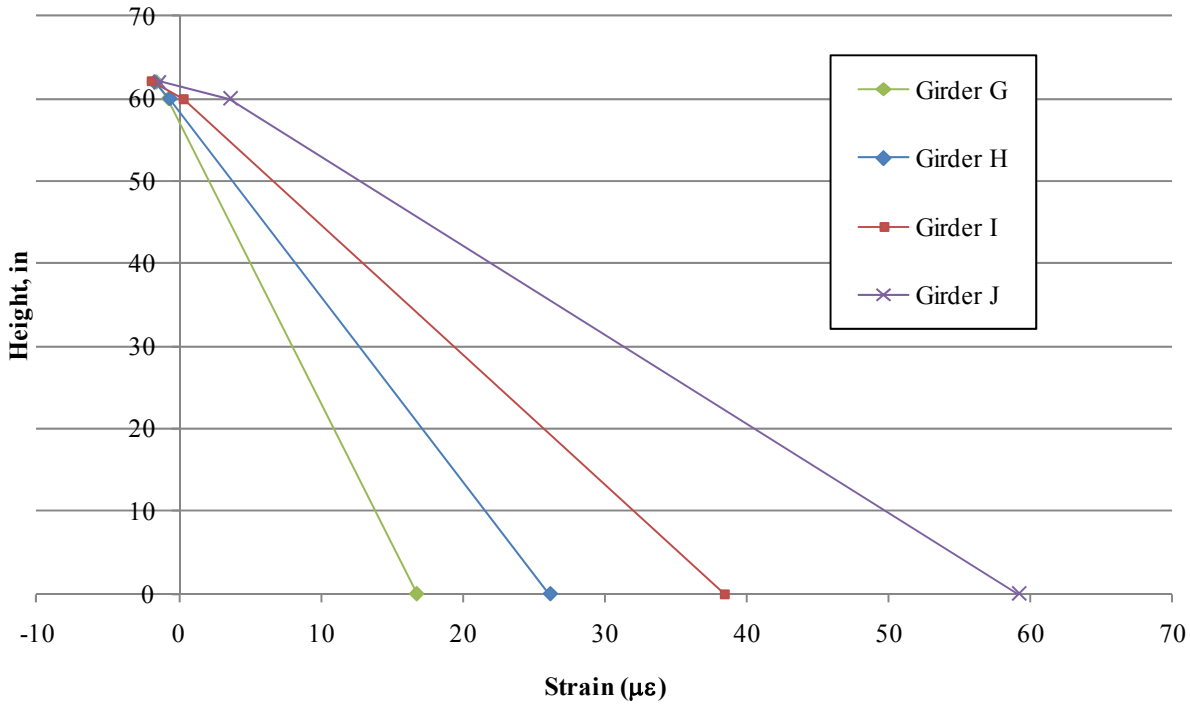

Figure 4.29. Strain depth profile for girders G through J, Load Case 2

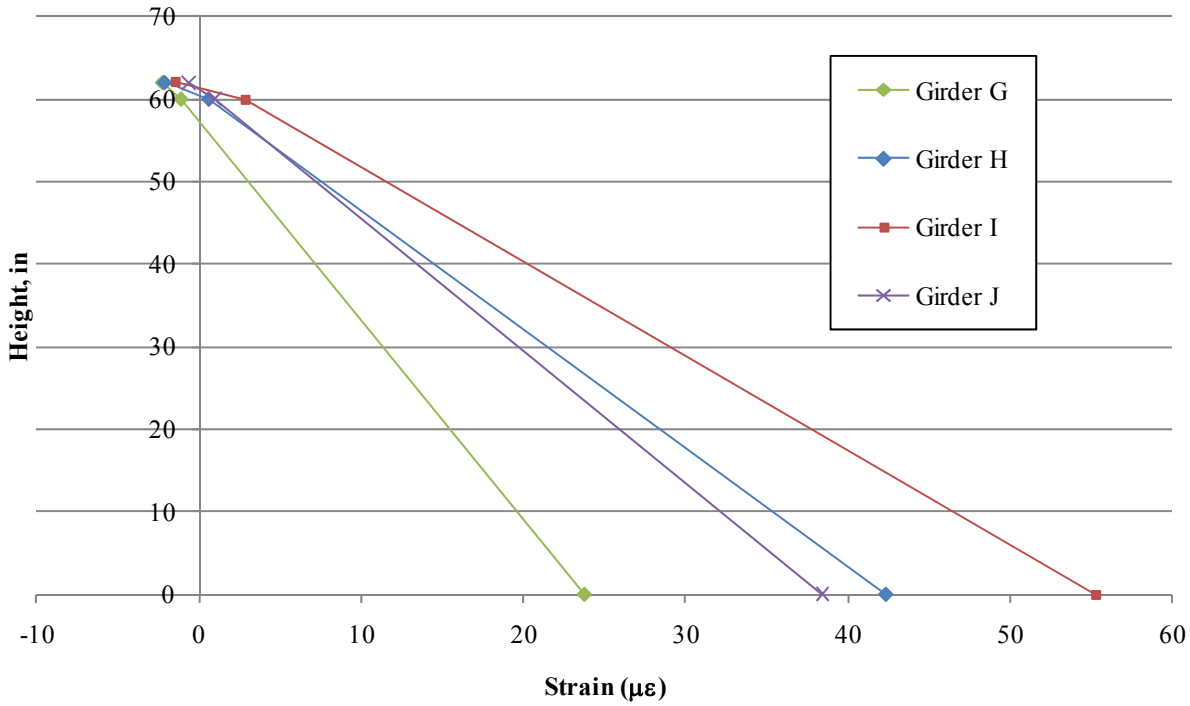

Figure 4.30. Strain depth profile for girders G through J, Load Case 3

4.5. Field Testing Key Findings

Four different field tests were performed to evaluate the performance of the 24th Street Bridge during construction and as a finished bridge. The test included monitoring strand corrosion, deck panel behavior during placement, post-tensioning strand behavior, and a diagnostic live load test. The following conclusions were made from the field testing:

1. All corrosion electrodes indicate that no corrosion is taking place in the strands.
2. During deck panel placement the peak strain in the panel was 230 με located at F2, which was near a pick point location.
3. Joint stress of 950 psi was observed in one of the load cells during the post-tensioning of the deck strands. It is uncertain, however, if the load cells were working properly.
4. The maximum north span deflection was observed to be -0.41 in., which corresponds to a span to deflection ration of L/5120.
5. The maximum strain of +66 με occurred at the midspan of girder L during LC1. The maximum strain range of 88 με occurred at the same location and load case.
6. The maximum strain range at the pier and abutment bottom flange locations were 19 με and 18 με respectively.
7. The closure pour differential movement was less than 0.04 in.
8. A maximum load fraction of 0.25 was seen at girder K during LC1.

9. The largest load distribution factor was found at girder H with a value of 0.63. The lowest load distribution factor of 0.30 occurred at girder A.
10. The load distribution factors obtained from field testing were within AASHTO LRFD load distribution requirements.
11. The neutral axis location obtained from field test was located between 58 in. and 61 in. form the bottom of the flange. The girder depth is 61 in.; therefore, the neutral axis lies near the top of the steel girder but not in the haunch or deck slab.

5. SUMMARY AND CONCLUSIONS

Using accelerated construction methods, a prestressed, precast bridge was constructed by the Iowa DOT. The design concept involved the use of precast deck components that were grouted compositely with the steel girders. The successful implementation of this approach has far reaching implications in Iowa as well as nationwide, as there are many instances where proven rapid construction techniques could result in significant reductions in costs.

The overall objective of this project was to assess bridge components and evaluate the overall performance of the 24th Street Bridge. In order to complete the objective the project included laboratory test and field testing. The laboratory test included evaluation of the shear stud pockets (including the stud bend test and grout flowability), evaluation of duct splicing performance, and the influence of surface treatment on transverse joint shear transfer. The field test included monitoring strand corrosion, deck panel behavior during placement, post-tensioning strand behavior, and a diagnostic live load test.

The following conclusions were obtained during the testing:

1. No difficulty in installing the shear studs in the precast panel pockets were foreseen by the contractor or encountered by the research team.
2. Conducting the bend test on the studs in the precast panel pockets was feasible for all six studs.
3. Grout with the proposed slump can sufficiently flow through the stud pockets into the haunch areas.
4. The waterproof duct tape and butyl rubber methods of grout proofing the duct splices were both acceptable.
5. Sandblasting the surface of the concrete/grout joint was the most effective surface treatment for resistance to shear.
6. All corrosion electrodes indicate that no corrosion is taking place in the strands.
7. During deck panel placement the peak strain in the panel was 230 με located at F2, which was near a pick point location.
8. Joint stress of 950 psi was observed in one of the load cells during the post-tensioning of the deck strands. It is uncertain, however, if the load cells were working properly.
9. The maximum north span deflection was observed to be -0.41 in., which corresponds to a span to deflection ration of L/5120.
10. The maximum strain of +66 με occurred at the midspan of girder L during LC1. The maximum strain range of 88 με occurred at the same location and load case.
11. The maximum strain range at the pier and abutment bottom flange locations were 19 με and 18 με respectively.
12. The closure pour differential movement was less than 0.04 in.
13. A maximum load fraction of 0.25 was seen at girder K during LC1.
14. The largest load distribution factor was found at girder H with a value of 0.63. The lowest load distribution factor of 0.30 occurred at girder A.

15. The load distribution factors obtained from field testing were within AASHTO LRFD load distribution requirements.
16. The neutral axis location obtained from field test was located between 58 in. and 61 in. form the bottom of the flange. The girder depth is 61 in.; therefore, the neutral axis lies near the top of the steel girder but not in the haunch or deck slab.

REFERENCES

AASHTO. 2004. *LRFD Bridge Design Specifications 2004*. Washington D.C.: American Association of State Highway and Transportation Officials.

Abu-Hawash, A., Hussein, K., McDonald, N., Phares, B., Schwarz, P., and Wipf, T., 2007. Accelerated Bridge Construction and Innovations, the 24th Street Bridge. National Steel Bridge Alliance 2007 World Steel Bridge Symposium.

Wipf, T., Klaiber, F., Phares, B., and Bowers, R. 2009. Precast Concrete Elements for Accelerated Bridge Construction: Laboratory Testing of Full-Depth Precast, Prestressed Concrete Deck Panels, Boone County Bridge. IHRB Project TR-561,CTRE Project 06-262. Iowa State University, Ames, IA.